

United Arab Emirates University

College of Engineering

WIRELESS ANTENNA MULTIPLEXING USING TUNABLE
ANTENNA FOR SPACE APPLICATIONS

Saifudeen Ahammed Kabeer

This dissertation is submitted in partial fulfilment of the requirements for the degree
of Doctor of Philosophy

Under the Supervision of Dr. Mahmoud F. Al Ahmad

April 2021

Declaration of Original Work

I, Saifudeen Ahammed Kabeer the undersigned, a graduate student at the United Arab Emirates University (UAEU), and the author of this dissertation entitled “*Wireless Antenna Multiplexing Using Tunable Antenna for Space Applications*”, hereby, solemnly declare that this dissertation is my own original research work that has been done and prepared by me under the supervision of Dr. Mahmoud F. Al Ahmad, in the College of Engineering at UAEU. This work has not previously formed the basis for the award of any academic degree, diploma or a similar title at this or any other university. Any materials borrowed from other sources (whether published or unpublished) and relied upon or included in my dissertation have been properly cited and acknowledged in accordance with appropriate academic conventions. I further declare that there is no potential conflict of interest with respect to the research, data collection, authorship, presentation and/or publication of this dissertation.

Student's Signature:  _____ Date: 19 April 2021

Copyright © 2021 Saifudeen Ahammed Kabeer
All Rights Reserved

Advisory Committee

1) Advisor: Dr. Mahmoud F. Al Ahmad

Title: Associate Professor

Department of Electrical Engineering

College of Engineering

2) Member: Dr. Falah Awwad

Title: Professor

Department of Electrical Engineering

College of Engineering

3) Member: Dr. Adel Najar

Title: Associate Professor

Department of Physics

College of Science

Approval of the Doctorate Dissertation

This Doctorate Dissertation is approved by the following Examining Committee Members:

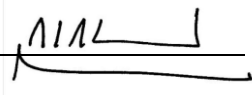
- 1) Advisor (Committee Chair): Dr. Mahmoud F. Al Ahmad

Title: Associate Professor

Department of Electrical Engineering

College of Engineering

Signature _____



Date April 29, 2021

- 2) Member: Dr. Qurban Ali Memon

Title: Associate Professor

Department of Electrical Engineering

College of Engineering

Signature _____



Date April 29, 2021

- 3) Member: Dr. Abderrahmane Lakas

Title: Professor

Department of Computer and Network Engineering

College of Information Technology

Signature _____



Date May 2, 2021

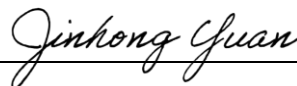
- 4) Member (External Examiner): Dr. Jinhong Yuan

Title: Professor

School of Electrical Engineering and Telecommunications

University of New South Wales, Sydney, Australia

Signature _____



Date May 3, 2021

This Doctorate Dissertation is accepted by:

Dean of the College of Engineering: Professor James Klausner

Signature James F. Klausner Date May 3, 2021

Dean of the College of Graduate Studies: Professor Ali Al-Marzouqi

Signature Ali Hassan Date August 3, 2021

Copy ____ of ____

Abstract

Recent development in the communication technologies shift the communication paradigm from point to point to multi user wireless system. These developments eased the use of mobile telephone, satellite services, 5G cellular, smart application, and the Internet of Things. The proliferation of mobile devices has necessitated an elaborate mechanism to serve multiple users over a shared communication medium, and multiplexing approach is introduced to serve this purpose. The multiplexing refers to a method which aims at combining multiple signals into one signal such that each user would be able to extract its desired data upon receiving the multiplexed signal. This spectrum sharing allows wireless operators to maximize the use of their spectrum to accommodate a large number of users over fewer channels. In Space applications, where sensors like temperature, attitude, IR, Magnetic etc. send information using antennas operates at different frequency, there is a need to collect all or some of these data using a single device. Wideband antenna requires a filtering process in order to remove unwanted signals that leads to a complex circuit design. Furthermore, the use of multiple antenna ends up with larger size and additional complexity. Therefore, tunable antenna is an excellent candidate which provides a perfect solution for such scenarios. A tunable antenna whose frequency characteristics shifted by applying tuning action can be used to operate as a multiplexing device that can collect signals from different surrounding antennas; each operates at fixed frequency. A system architecture for wireless multiplexing using tunable antenna is proposed in this project. An electronically tunable antenna using varactor diode as tuning element used as the multiplexing device that can collect signals from different surrounding antennas. The system consists of RF front end and a control circuit/system for wireless multiplexing. The RF front end consists of a tunable antenna, tunable phase shifter, tunable band pass filter, low noise amplifier, mixer, voltage-controlled oscillator and an intermediate frequency filter. The control unit comprises a microcontroller, DAC, CMOS oscillator, power module and a USB interface for communication with a custom-built software installed on a PC. The device has functions for control, digital signal processing and de-multiplexing. The device is fed with an input multiplexed signal, and the de-multiplexed output signals are extracted and displayed on the graphical user interface of the software. Due to the re-configurability and

programmability of the device, it presents a flexible, cost effective solution for a variety of real-world applications.

Keywords: Wireless multiplexing, reconfigurability, tunable antenna, smart systems, space communications, varactor diode, information technology.

Title and Abstract (in Arabic)

امسك الاشارات اللاسلكية باستخدام الهوائي القابل للضبط لتطبيقات الفضاء

الملخص

أدى التطور الأخير في تقنيات الاتصالات إلى تحويل نموذج الاتصال من نقطة إلى أخرى إلى نظام لاسلكي متعدد المستخدمين. سهلت هذه التطورات استخدام الهاتف المحمول، وخدمات الأقمار الصناعية، والجيل الخامس والتطبيقات الذكية، وإنترنت الأشياء. استلزم تكاثر الأجهزة المحمولة آلية معقدة لخدمة مستخدمي متعددين عبر وسيط اتصال مشترك، وتم تقديم نهج تعدد الإرسال لخدمة هذا الغرض. يشير تعدد الإرسال إلى طريقة تهدف إلى الجمع بين إشارات متعددة في إشارة واحدة بحيث يكون كل مستخدم قادرًا على استخراج البيانات المطلوبة عند استقبال الإشارة متعددة الإرسال. يسمح تقاسم الطيف هذا لمشغلي الشبكات اللاسلكية بتعظيم استخدام الطيف الخاص بهم لاستيعاب عدد كبير من المستخدمين عبر عدد أقل من القنوات. في التطبيقات الفضائية، حيث ترسل أجهزة الاستشعار مثل درجة الحرارة، والموقف، والأشعة تحت الحمراء، والمغناطيسية، وما إلى ذلك معلومات باستخدام هوائيات تعمل بتردد مختلف، هناك حاجة لجمع كل هذه البيانات أو بعضها باستخدام جهاز واحد. يتطلب هوائي النطاق العريض عملية ترشيح لإزالة الإشارات غير المرغوب فيها التي تؤدي إلى تصميم دائرة معقدة. علاوة على ذلك، فإن استخدام هوائي متعدد ينتهي بحجم أكبر وتعقيد إضافي. لذلك، يعد الهوائي القابل للضبط مرشحًا ممتازًا يوفر حلاً مثاليًا لمثل هذه السيناريوهات. يمكن استخدام الهوائي القابل للضبط الذي تغيرت خصائص تردده من خلال تطبيق إجراء التوليف للعمل كجهاز تعدد إرسال يمكنه تجميع الإشارات من الهوائيات المحيطة المختلفة؛ كل يعمل بتردد ثابت. تم اقتراح بنية نظام لتعدد الإرسال اللاسلكي باستخدام هوائي مضبوط في هذا المشروع. هوائي قابل للضبط إلكترونيًا يستخدم الصمام الثنائي المتغير كعنصر ضبط يُستخدم كجهاز تعدد إرسال يمكنه جمع الإشارات من الهوائيات المحيطة المختلفة. يتكون النظام من واجهة (RF) الأمامية ودائرة / نظام تحكم لتعدد الإرسال اللاسلكي. تتكون الواجهة الأمامية للتردد اللاسلكي من هوائي مضبوط، ومبدل طور قابل للضبط، ومرشح تمرير نطاق قابل للضبط، ومضخم منخفض الضوضاء، وخلاط، ومذبذب متحكم في الجهد، ومرشح تردد وسيط. تتكون وحدة التحكم من متحكم دقيق و (DAC) ومذبذب (CMOS) ووحدة طاقة وواجهة (USB) للاتصال ببرنامج مصمم خصيصًا مثبتًا على جهاز كمبيوتر. يحتوي الجهاز على وظائف للتحكم ومعالجة الإشارات الرقمية وإلغاء الإرسال المتعدد. يتم تغذية الجهاز

بإشارة مدخلات متعددة، ويتم استخراج إشارات الإخراج غير المضاعفة وعرضها على واجهة المستخدم الرسومية للبرنامج. نظرًا لإعادة تكوين الجهاز وإمكانية برمجته ، فإنه يقدم حلاً مرثاً وفعالاً من حيث التكلفة لمجموعة متنوعة من تطبيقات العالم الحقيقي.

مفاهيم البحث الرئيسية: مضاعفة الإرسال اللاسلكي، إعادة التكوين، الهوائي القابل للضبط، الأنظمة الذكية، الاتصالات الفضائية، الصمام الثنائي المتغير، تكنولوجيا المعلومات.

Acknowledgements

Alhamdulillah, I praise and thank Allah SWT for his greatness and for giving me the strength and courage to complete this dissertation.

First and foremost, I am extremely grateful to my supervisor, Dr. Mahmoud F. Al Ahmad for his precious advice, continuous support, and patience during my PhD journey. I would also like to thank my advisory committee members, Dr. Falah Awwad and Dr. Adel Najjar for their valuable suggestions on my study and research. I would like to thank all the faculty members in the Electrical Engineering Department for assisting me all over my studies and research. My special thanks are extended to the laboratory specialists Eng. Mutaz Mohamed and Eng. Abdulrahman Daher for their help during the fabrication process of the antenna. I would like to extend my gratitude towards my research team members specially Dr. Lillian Among. I would like to acknowledge the National Space Science and Technology Center, UAE University for providing the funds for my PhD research. Many thanks go for Dr. Khaled Al Hashmi (Center Director) and Dr. Omar Imam (Center technical leader) for their continuous help and support.

I would like to express my gratitude to my parents, sisters. Without their tremendous understanding and encouragement in the past few years, it would be impossible for me to complete my study.

Finally, I would like to thank each and every one who was important to the successful realization of this dissertation, as well as expressing my apology that I could not mention personally one by one.

Dedication

To my beloved parents and family

Table of Contents

Title	i
Declaration of Original Work	ii
Copyright	iii
Advisory Committee	iv
Approval of the Doctorate Dissertation	v
Abstract	vii
Title and Abstract (in Arabic)	ix
Acknowledgements	xi
Dedication	xii
Table of Contents	xiii
List of Tables	xv
List of Figures	xvi
List of Abbreviations	xviii
Chapter 1: Introduction	1
1.1 Overview	1
1.2 Statement of the Problem	2
1.3 Dissertation Objective	5
1.4 Dissertation Outline	5
Chapter 2: State of Art	6
2.1 Multiplexing and Wireless Technologies	8
2.1.1 Time Division Multiplexing (TDM)	10
2.1.2 Frequency Division Multiplexing (FDM)	11
2.1.3 Orthogonal Frequency Division Multiplexing (OFDM)	13
2.1.4 Code Division Multiplexing (CDM)	14
2.1.5 Wavelength Division Multiplexing (WDM)	15
2.1.6 Polarization Division Multiplexing (PDM)	16
2.2 Tunable Antenna	17
2.2.1 Electrically Tunable Antenna	19
Chapter 3: Wireless Multiplexing Agile Antenna-based Control System	29
3.1 Proposed Solution	29
3.2 Biasing Overview	30
3.3 Wireless Antenna Multiplexer (WAM) Unit Blocks	32
3.3.1 PIC	32
3.3.2 Digital to Analog Converter (DAC)	33
3.3.3 Universal Serial Bus (USB) Interface	33

3.3.4 Oscillator	34
3.3.5 Power Module	34
3.3.6 WAM Application.....	34
3.3.7 Indicator LEDs	35
3.3.8 Input Ports	35
3.3.9 Output Ports	35
3.4 Device Operation	35
3.5 Measurement Setup.....	37
3.6 Results and Discussion	38
Chapter 4: Compact Frequency Reconfigurable Microstrip Patch Antenna.....	42
4.1 Proposed Design Overview.....	42
4.2 Frequency Reconfigurable Antenna Design and Simulation.....	42
4.3 Antenna Experimental Setup and Measurement.....	52
4.4 Reflection Coefficient Measurements and Analysis.....	52
4.5 Far-Field Measurements and Analysis.....	56
Chapter 5: Outlook and Conclusions	63
5.1 Conclusions	63
5.2 Outlook	64
References.....	67
List of Publications	74

List of Tables

Table 1: Approaches for Antenna Multiplexing	8
Table 2: Comparison of electrically tunable methods	26
Table 3: Comparison between simulated and measured resonant frequency	56
Table 4: Comparison of proposed design with reported works employing varactor diodes	61

List of Figures

Figure 1: Need for Antenna Multiplexing	3
Figure 2: Synchronous TDM	11
Figure 3: Asynchronous TDM	11
Figure 4: Frequency division multiplexing.....	12
Figure 5: Use of guard bands in FDM	12
Figure 6: Orthogonal frequency division multiplexing	14
Figure 7: Multiple access methods	15
Figure 8: Wavelength division multiplexing	16
Figure 9: Frequency tuning techniques.....	18
Figure 10: Wireless antenna multiplexing system.....	30
Figure 11: Quantized waveform (a) rectified sinusoidal wave (b) saw tooth wave	31
Figure 12: Multiple device biasing	32
Figure 13: Wireless Antenna Multiplexing (WAM) board.....	33
Figure 14: WAM system board operational block diagram.....	36
Figure 15: Measurement Setup	38
Figure 16: DC power supply to the board.....	38
Figure 17: Plot of de-multiplexed input signal $S(t)$ in the WAM application	39
Figure 18: Board configuration settings	39
Figure 19: Voltages at pins V_0 and V_1 measured using an oscilloscope.....	40
Figure 20: Voltages at pins V_2 and V_3 measured using an oscilloscope.....	41
Figure 21: Voltages at pins V_4 and V_5 measured using an oscilloscope.....	41
Figure 22: Evolution of the reconfigurable antenna design.....	44
Figure 23: Return loss and resonant frequency shift with antenna evolution simulation results from CST	45
Figure 24: Antenna structure with dimensions	45
Figure 25: Equivalent model for SMV1234 varactor diode	47
Figure 26: Tuned capacitance versus applied voltage of the SMV1234.....	47
Figure 27: Variation in CST simulated reflection coefficient for different applied DC voltage bias levels.....	48
Figure 28: Electromagnetic field distribution at zero bias for (a) xy plane at $z = 1.67$ mm and (b) xz planes at $y=0$ mm.....	49
Figure 29: Frequency reconfigurable antenna equivalent circuit.....	50
Figure 30: Comparison of resonant frequency from CST simulation and circuit model with corresponding percentage error	51
Figure 31: CST simulation results of axial ratio versus θ at $\Phi = 0$ for varying bias voltages.....	51
Figure 32: Reflection coefficient measurement (a) measurement setup with the vector network analyzer (b) the Bias Tee connection.....	53

Figure 33: Fabricated antenna (a) perspective view of top (b) perspective view of ground showing inductive pin.....	53
Figure 34: Antenna under test on Roll-over-Azimuth positioner in anechoic chamber at IMST	54
Figure 35: Frequency reconfigurable antenna measured reflection coefficient versus frequency for different applied DC bias voltage levels	55
Figure 36: Normalized gain radiation pattern of the antenna at zero bias	59
Figure 37: Normalized absolute gain radiation patterns plots	60

List of Abbreviations

ADC	Analogue to Digital Converter
BST	Barium Strontium Titanate
CDM	Code Division Multiplexing
CDMA	Code Division Multiple Access
DAC	Digital to Analogue Converter
FDM	Frequency Division Multiplexing
FFT	Fast Fourier Transform
LED	Light Emitting Diode
MEMS	Micro Electro Mechanical Switch
MIMO	Multi Input Multi Output
OFDM	Orthogonal Frequency Division Multiplexing
OFDMA	Orthogonal Frequency Division Multiple Access
PDM	Polarization Division Multiplexing
PIC	Peripheral Interface Controllers
QAM	Quadrature Amplitude Modulation
QPSK	Quadrature Phase shift Keying
RF	Radio Frequency
SDMA	Space Division Multiple Access
SFN	Single Frequency Networks
TDM	Time Division Multiplexing
USB	Universal Serial Bus
WAM	Wireless Antenna Multiplexing
WDM	Wavelength Division Multiplexing

Chapter 1: Introduction

1.1 Overview

Today wireless becomes the pioneer in communication system. Wireless technologies like Wi-Fi, ZigBee, Bluetooth, Radio Frequency Identification tags (RFIDs), WiMAX, and satellite communication etc. are revolutionized the communication system and modern society. The rapid growth of mobile telephone use, various satellite services, 5G cellular, and the Internet of Things (IoT) are generating tremendous changes in telecommunications and networking field. With these advancements, the communication system has moved from one to one system to multi-customer wireless networks in order to accommodate the growing number of mobile devices. The rise of mobile devices has demanded an elaborate mechanism called multiplexing to serve multiple users over a common communication channel. The Multiplexing is a technique for combining multiple analog or digital signals into a single signal over a shared medium such that user can able to recover the desired signal at the receiver end through demultiplexing. This spectrum sharing allows wireless operators to maximize the use of their spectrum to accommodate a large number of users over fewer channels. Technologies based on multiplexing like multi input multi output (MIMO), orthogonal frequency division multiplexing (ODFM), orthogonal frequency division multiple access (OFDMA) are the backbone behind the modern wireless technologies. In a multiplexed system user requirement are ordinarily fixed, in multiple access system user allocation can dynamically change with time. The steady growth and increment in communication services and applications calls for the implementation and utilization of dynamic and reconfigurable communication approaches; agile based frequency reconfiguration should be considered. A set of

antenna operates at different frequency communication link/bandwidth are transmitting data (for example sensory data) in the space, there is a need to collect all or some of these transmitted signals by a single device. Wireless multiplexing using tunable antenna can serve this purpose. A tunable antenna whose frequency characteristics shifted by applying tuning action can be used to operate as a multiplexing device that can collect signals from different surrounding antennas; each operates at fixed frequency.

1.2 Statement of the Problem

Wireless capacity is expected to increase by more than one thousand within couple of years. This calls for joint efforts from different discipline to develop smart technologies. The steady growth and increment in communication services and applications, demands for the reconfigurable communication approaches; mainly frequency reconfiguration. In Space or satellite applications, there are different sensory satellite nodes operates at different frequencies that are responsible to collect data for space/earth observation and communicate directly with the main central satellite. A receiver in the main satellite in turns collects the data and send directly to ground station. Consider the scenario as shown in the Figure 1, there are four sensory satellite nodes operating at different frequencies f_0 , f_1 , f_2 and f_3 .and all of the sensory information has to be collected by the receiver in the main satellite. Antenna is one the main element of the communication system and which are responsible for transmission and reception of the signals. The receiver in the antenna should have the capability to collect all of those signals. In order to receive the signal from specific satellite antenna, the resonance frequency of the main satellite has to be identical to that of the transmitting antenna.

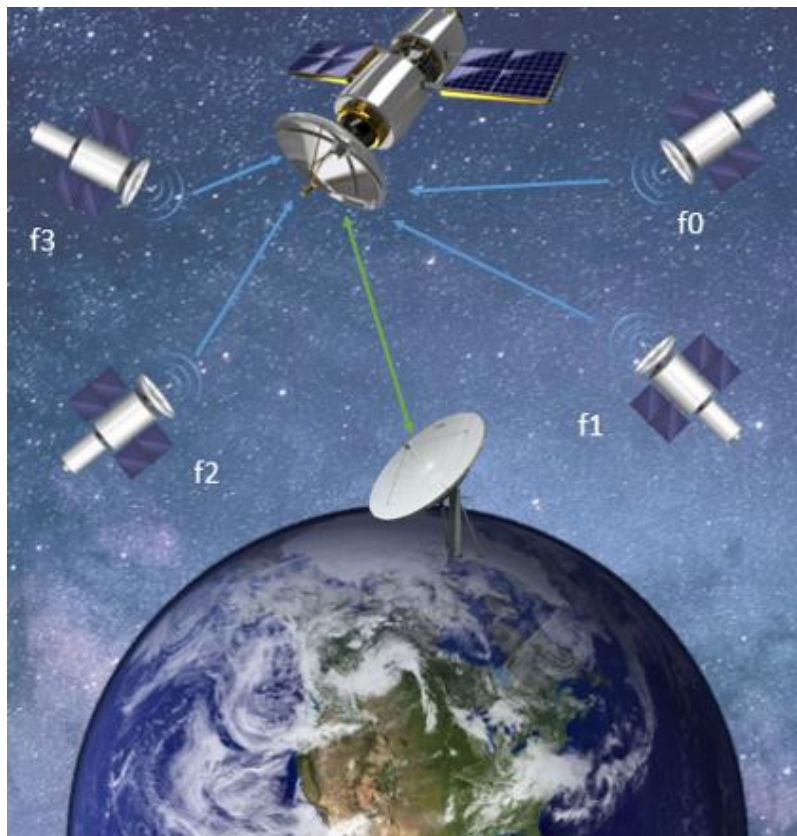


Figure 1: Need for Antenna Multiplexing

There are three possible solutions for this scenario. In the first approach for signal reception, multiple antennas are used, with each antenna supporting just one frequency. This arrangement has excellent individual radio performances and allows for simpler front-end design and looser filter requirements [1]. However, since the number of antennas needed is dependent on the number of frequency bands or services, receiver based on multiple antennas ends up with larger size and further complexity. Also due to larger cabling requirement multiple antenna approach is quite expensive. Thus, there is emerging need for a smart and efficient antenna solutions. In the second approach wide band or multiband antenna solutions are used which reduces the space requirements. In this case a single antenna can support all frequency bands or services. The method necessitates a large number of stringent filters in the front end, which

increases insertion loss and, as a result, decreases receiver sensitivity [1]. Even though dedicated single-band antennas can offer superior efficiency, multiband antennas, which are built to address more than one band/service at a time, are currently the most feasible and inexpensive single wireless module solution. Multiband antennas, on the other hand, face significant challenges as more wireless networks are crammed into ever-smaller devices. In order to avoid the requirement of stringent filters at the RF front end for multiband antenna, a dynamic and reconfigurable approach named frequency tunable antennas are introduced, which is the third and most appropriate solution for such scenarios. In this case, a single antenna can cover a wide range of wireless standards by changing its frequency characteristics from one frequency to another in response to a tuning action such as electrical, mechanical, optical or material change [2]. In electrical method, tuning elements are introduced in to the antenna structure such as PIN diode, varactor diode, FET etc. and voltage is applied to change the resonance frequency. Although there is some additional cost for the tuning element, the approach has less space requirements, reasonable efficiency, and a more relaxed filter specification. To summarize, most multiband antenna solutions necessitate the use of very costly stringent filters to increase out-of-band rejection. Frequency-tunable antennas, on the other side, have built-in band pass characteristics and, without the use of filters, have outstanding out-of-band rejection [1]. Higher-order resonances can exist in tunable antennas, but they are usually located far away from the operating band which can be removed by simple low-cost band-pass filters.

If the tunable antenna based wireless multiplexing system is installed on the main satellite it will replace several antenna elements and processing unit, which will result in compact, lighter weight and rapid data processing.

1.3 Dissertation Objective

The objective of the present work is to develop a wireless multiplexing system architecture using a tunable antenna. The work mainly includes the design, fabrication and testing of two main components, a control unit for wireless antenna multiplexing system and tunable antenna based on electrical method. The proposed system is designed to operate between 1 to 2 GHz.

1.4 Dissertation Outline

The dissertation in the following sections composed of five main chapters. In the second chapter, a state of art about various multiplexing techniques and related tunable antenna works has been investigated. In Chapter 3, Wireless Multiplexing Agile Antenna-based Control System is introduced in detail. WAM design, block diagrams, components, measurements, results and discussions are explained in this section. Compact tunable patch antenna design, simulations and measurement results were analyzed in Chapter 4 along with a comparison with the previously reported work. Outlook and conclusion including future works are discussed in the Chapter 5.

Chapter 2: State of Art

The concept of multiplexing arose as a mechanism for allowing multiple users to efficiently utilize a limited, shared communication medium. Multiplexing refers to a method where by several signals at the transmitting side of a communication system are combined into one signal for transmission. At the receiving end, each user is able to extract their desired data reliably from the multiplexed signal. In communication systems, antennas are responsible for transmission and reception of signals [3]. The steady growth and increment in communication services has led to the increase in number of antennas [1] used to cover the different frequency communication link/bandwidth as these antennas mostly operate at a fixed frequency.

There are three main approaches to antenna multiplexing. In the first approach, multiple antennas are used for signal reception, with each antenna supporting only a single frequency or service. This arrangement allows for simpler front-end design and looser filter specifications and has excellent individual radio performance. The limitation of this approach however is that since the number of antennas depends on the number of frequency bands, services and diversity required, the overall system might have large space requirements as close spacing between antennas can result in strong coupling between radios. This approach also has high cost due to the cabling requirements for each of the antennas [1]. An alternative approach is to use multiband [3-5] or wide band antennas [6-8]. This is where a single antenna supports all frequency bands or services. As such, it has a lower space requirement. One drawback of this approach is that the wide bandwidth puts limits on the amount of miniaturization possible. The approach also requires many stringent filters in the front end, which increases insertion loss, which in turn reduces the receiver sensitivity. The stringent

filter requirement also drives up the cost of the approach. The third approach is to utilize dynamic and reconfigurable approaches such as a frequency reconfigurable (tunable/agile) antennas [2, 9, 10]. This is where a single antenna can support many wireless standards. It does so by switching its frequency characteristics on application of a tuning action such as voltage or mechanical force. The antenna can receive from a specific antenna by adjusting its resonance frequency to be identical that of the transmitting antenna. Alternatively, by switching its frequency characteristics with high speed, it can receive signals over a wide spectrum, covered by several transmit antennas in the communication link. The tuning speed of the antenna can be adjusted evenly to receive and recover the data practically simultaneously and instantaneously. Although there is some additional cost for the tuning element, the approach has reduced space requirements, acceptable performance and relaxed filter specification [1]. The three possible antenna multiplexing approaches are summarized in Table 1.

As explained in the Table 1, tunable antennas are excellent solution for wireless communication applications. Commercial solutions are available for the first two approaches [11, 12], however to the best of these authors knowledge, there is no commercially available solution, or proposed literature that utilizes a frequency tunable/agile antenna. Designing a frequency tunable antenna based wireless multiplexing system is still a challenging question. It requires several stages of design process and individual and combined performance testing of components. The tunable antenna based wireless multiplexing system needs a tunable antenna, RF front end and control unit.

Table 1: Approaches for Antenna Multiplexing

Multiple Antenna	Wideband/Multi band antenna	Tunable Antenna
Individual Antenna for each frequency	A single antenna supports all frequency bands or services	A single antenna can support many wireless standards by the application of tuning action.
Simpler front-end design and looser filter specifications	Lower space requirement	Has reduced space requirements, acceptable performance and relaxed filter specification
Overall system might have large space requirements	Filter requirement	Good isolation between adjacent frequencies
Close spacing between antennas can result in strong coupling between radios	Amount of miniaturization is limited	Multifunctional capabilities
High cost due to the cabling requirements for each of the antennas'	Increased insertion loss	Additional cost for tuning element and its biasing

2.1 Multiplexing and Wireless Technologies

Today wireless is becoming the leader in communication choices among users. Wireless technology is no longer a contingency option for nomads, but rather a new mood that is instinctively adopted everywhere, even when wired communications are available. Multiplexing and multiple access are the backbone of these wireless technologies.

In 1993, Arogyaswami Paulraj and Thomas Kailath introduced a Space-division multiple access SDMA-based reverse multiplexing technique to increase the capacity of the wireless broadcasting system from a central studio to a multitude of

users in a service area [13]. The high-rate signal is divided into several low-rate signals to be transmitted from "spatially separated transmitters" and recovered by the receiving antenna array based on variations in "directions of arrival" so that it can be accommodated within the bandwidth allocated. Idea of using multiple antennas at both the transmitter and receiver along with MIMO applications are introduced by Arogyaswami Paulraj. Current high-speed Wi-Fi and 4G mobile systems are based on this theory. Robert W. Chang introduced OFDM concept, it is a frequency-division multiplexing technique in which a large number of closely spaced orthogonal subcarriers are transmitted in parallel [14]. The use of FFT in frequency division multiplexing was introduced by Weinstein and Ebert in 1971 [15]. This work also discusses about the use of guard interval to reduce the interference among sub channels. An OFDM-based Digital Audio Broadcasting standard was introduced in 1995. OFDM allows a network of transmitters to operate at same transmission frequency while providing a large coverage area this enables the use of single-frequency networks (SFN). OFDMA was proposed by Sari and Karam for cable television networks [16], which combines the OFDM and frequency division multiple access techniques. by adjusting FFT size to channel bandwidth and fixing the sub-carrier frequency spacing ratio, Scalability is achieved in OFDMA structures. In OFDMA multiple access is accomplished by assigning subcarrier subsets to individual users. This enables low data-rate transfer from multiple users at the same time.

A multiplexer is an important component of many microwave front-end systems like in radar,5G and other communication purposes. Different types of multiplexing are introduced in different literature and different implementation schemes are developed. Multiplexing is broadly classified into analogue and digital multiplexing and which is further divided into many sub categories.

2.1.1 Time Division Multiplexing (TDM)

Time division multiplexing is the oldest multiplexing scheme in which all the users are given the total spectral medium on a time-sharing basis. It is basically a digital multiplexing method where signals from different sources share the full bandwidth in a non-overlapping scheme like round robin algorithm. With TDM, each channel gets all of the bandwidth periodically during brief intervals of time. Buffer, Multiplexer, Modulator are the main components in the transmitter and demodulator, demultiplexer and buffer are used at the receiver. TDM is further classified in to synchronous or asynchronous mode. In synchronous TDM A fixed time slot is assigned to different users in a predefined order, no matter if some sources have no information to send, which degrades the throughput of the system. A typical synchronous TDM system is shown in Figure 2, and frame is divided into n time slot and for every user one slot is allocated. Synchronizing various data sources is the main issue in TDM. Pulse stuffing is often used as a means of controlling synchronization in systems that require both transmitter and receiver to transmit at the same bit rate. If there are n users, then the frame is divided into n time slot and for every user one slot is allocated. Same clock input is used such that the sampling rate is common for all.

In order to avoid these limitations of asynchronous mode is introduced in which the time slots are dynamically allocated to the users according to demand. If the allotted user for a time slot transmits has nothing to send, then that slot can be allocated to another user to improve the throughput as shown in Figure 3. Asynchronous TDM is also known as statistical TDM. Statistical TDM is the base for Packet Switching. TDM is implemented in different applications like synchronous digital hierarchy

(SDH)/synchronous optical networking (SONET), Integrated Services Digital Network (ISDN).

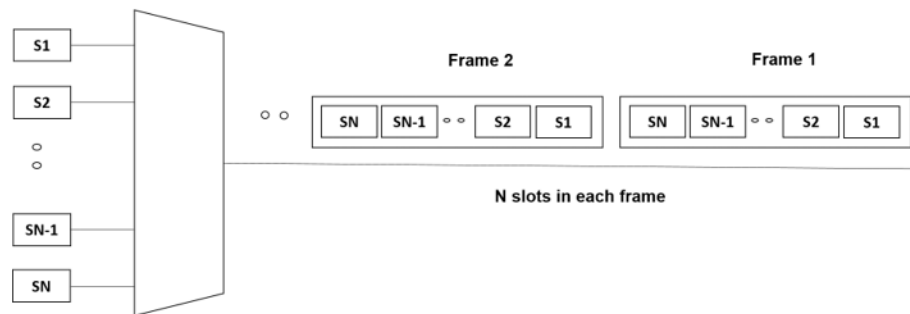


Figure 2: Synchronous TDM

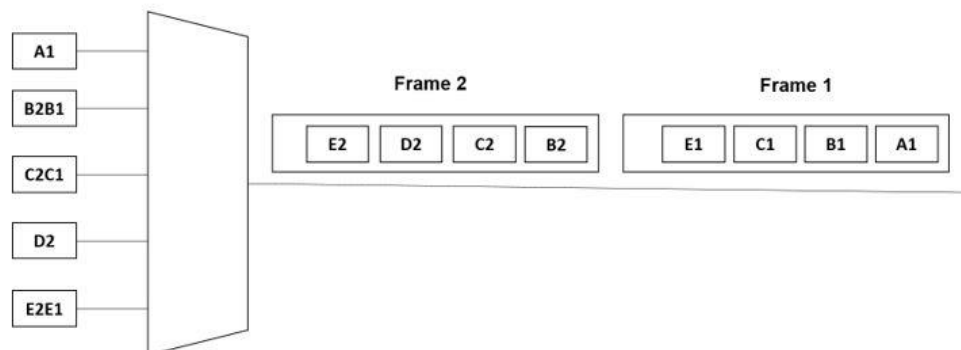


Figure 3: Asynchronous TDM

2.1.2 Frequency Division Multiplexing (FDM)

Frequency division multiplexing is an analogue multiplexing scheme in which available bandwidth is separated into multiple sub-bands each of which is able to carry a signal such that concurrent transmission is possible. In FDM, number of signals are

carried simultaneously on the same medium and each signal is modulated to a different carrier frequency at transmitter and demodulated accordingly at receiver. A typical FDM system is depicted in Figure 4, all the modulated signals are combined to form a composite multiplexed signal. Carrier frequencies are separated by guard bands to ensure non-overlapping of data as shown in Figure 5. FDM is used in FM radio, CATV, cellular networks, wireless networks and for satellite communications.

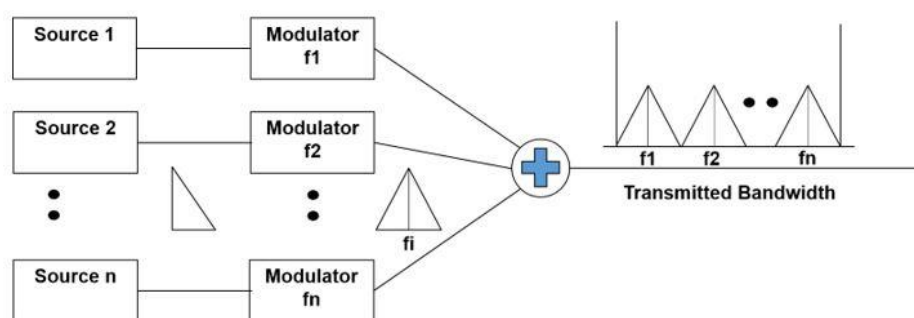


Figure 4: Frequency division multiplexing

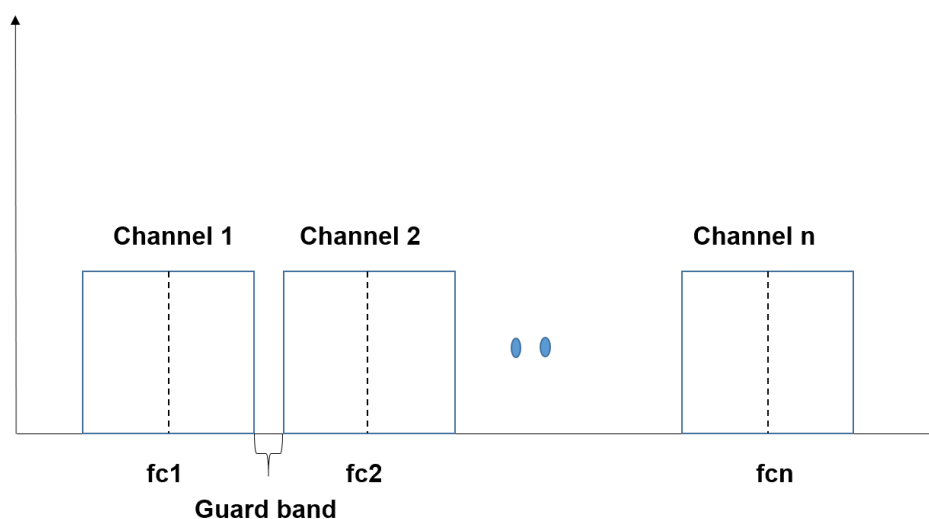


Figure 5: Use of guard bands in FDM

2.1.3 Orthogonal Frequency Division Multiplexing (OFDM)

Orthogonal Frequency Division Multiplexing (OFDM) falls under frequency-division multiplexing technique in which a large number of closely spaced orthogonal subcarriers are transmitted in parallel. Basic approach of OFDM is illustrated in Figure 6. The orthogonality of this technique is offered by the spacing, and which prevents the demodulators from seeing frequencies other than their own. Quadrature amplitude modulation (QAM), Quadrature Phase Shift Keying (QPSK) or similar modulation schemes are used to modulate the subcarriers. Combination of low symbol rate of subcarrier gives equivalent data rate. FFT and IFFT algorithms makes implementation of OFDM easier. Features like immunity to selective fading, resistance to interference, spectrum performance, resistance to ISI, and reasonable computational complexity, makes OFDM particularly common in broadband wireless communication systems.

Compared to traditional FDM, OFDM uses Multiple carriers to carry the information stream, and these subcarriers are orthogonal to each other, and reduced channel delay spread and inter symbol interference with the addition of guard intervals. FFT and IFFT helps to map digitally modulated input data to orthogonal subcarriers. In principle, the IFFT takes frequency-domain input data and converts it to the time-domain output data. OFDM is a widely used in wireless LAN and MAN applications, including IEEE 802.11a/g/n standards and WiMAX.

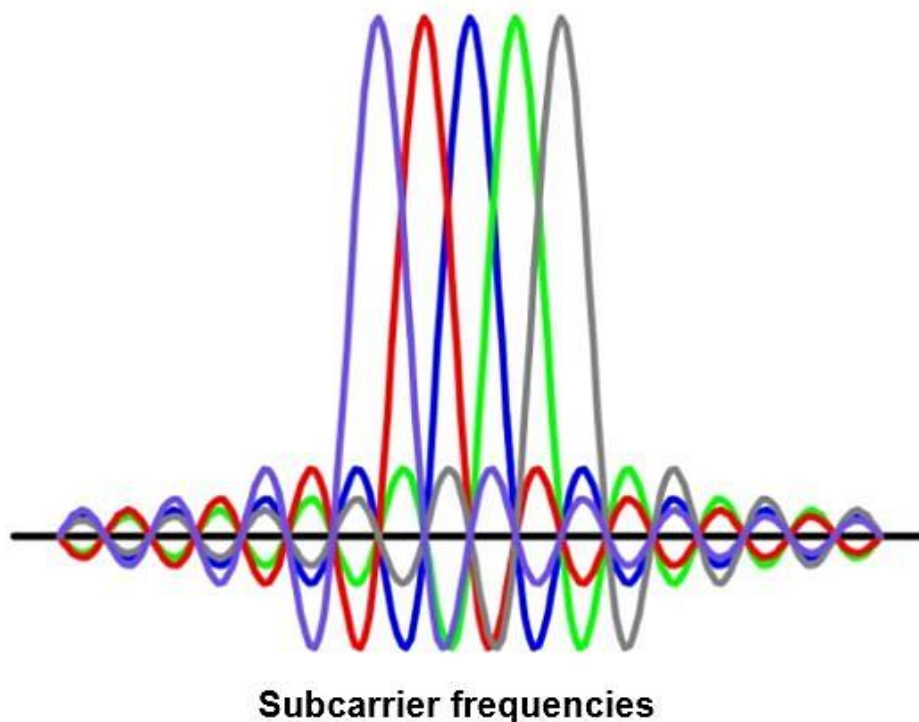


Figure 6: Orthogonal frequency division multiplexing

2.1.4 Code Division Multiplexing (CDM)

Code division multiplexing (CDM) is a multiplexing technique based on spread spectrum communication. It takes full advantage of the bandwidth available. A narrowband signal is distributed across a wider frequency band or across several channels. In CDM, the multiplexer assigns a separate code from a series of orthogonal pseudo random sequences to each user and at receiver original signal is recovered using the orthogonality property. Different multiple access technologies are depicted in Figure 7. CDMA can be implemented in several ways, two of which are frequency hopping and direct sequencing.

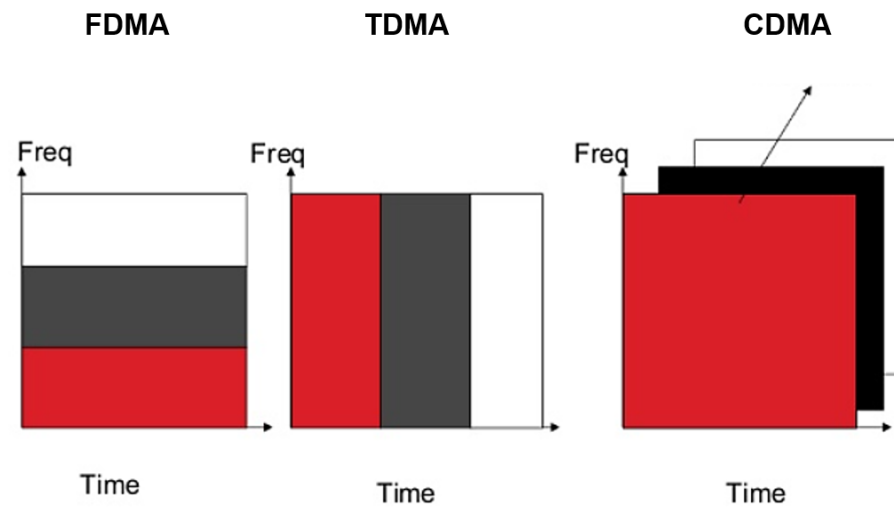


Figure 7: Multiple access methods

CDMA is used as the access method in many mobile cell phone standards, including cdma2000, W-CDMA, TD-CDMA etc. CDM is less susceptible to interference, thus providing better data communication capability and a more security along with soft handoff.

2.1.5 Wavelength Division Multiplexing (WDM)

In optical fiber communication, wavelength-division multiplexing (WDM) is used when a number of optical carrier signals are multiplexed on a single optical fiber with varying wavelengths of laser light. WDM expand the capacity of the network without laying more fiber. Actually, the capacity of a given link is expanded simply by upgrading the multiplexers and demultiplexers at each end. The Multiplexing and demultiplexing process of light signals can be explained with the help of a prism as shown in Figure 8. By integrating lights with various wavelengths from different sources, one prism acts as a multiplexer and the combined signal can be sent over long

distances using an optical fiber cable. At the receiver cable the combined signal is demultiplexed in to individual signals through another prism.

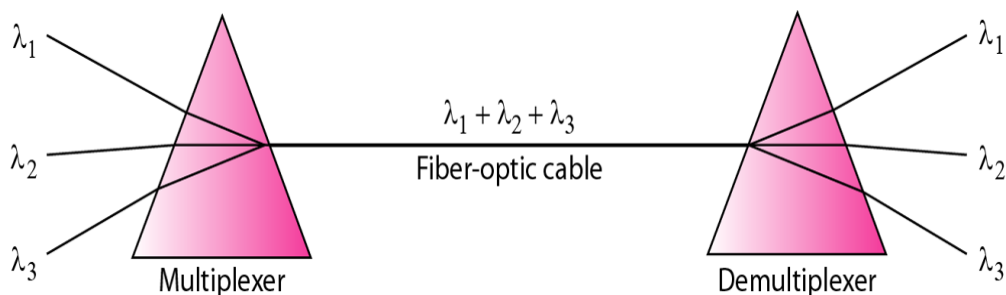


Figure 8: Wavelength division multiplexing

2.1.6 Polarization Division Multiplexing (PDM)

Polarization-division multiplexing (PDM) is a type of physical layer multiplexing technique which uses waves of two orthogonal polarization states to enable two channels of information to be transmitted on the identical carrier frequency. PDM is used in satellite television downlink to doubles the bandwidth and fiber optic communication by using two orthogonally polarized feed antennas and by transmitting left and right circularly polarizes light beams respectively.

There have been several attempts to build different forms of multiplexers using PIN diode, mechanical switches, active filters, dielectric filters, ferrite, coaxial filters. Multiplexers using passive hybrid microstrip filters has gain more popularity due to simplicity and reliability. However, they suffer from parasitic passband. Antenna multiplexing concept of switching between multiple antennas connected to a single TRF7970A NFC transceiver IC is discussed by Texas Instruments Inc. [11]. To multiplex antennas, it is necessary to switch between the antennas and to identify the

antenna used. To keep the complexity of the design low, a low power loss switch with simple control methods has been used. Wang designed a microstrip multiplexer from 10 to 21 GHz which can be used in for broadband system applications [17]. The multiplexer consists of four microstrip band pass filters with center passband frequencies at 10, 12, 19, and 21 GHz. The system comprises of two dedicated channels for the receiver and transmitter.

2.2 Tunable Antenna

Tunable or reconfigurable antenna has the capability to change the antenna parameters like frequency characteristics, polarization, or radiation pattern characteristics through the application of some tuning action. Based on this tunable antenna are classified into frequency tunable antenna, radiation pattern reconfigurable antenna, polarization reconfigurable antenna and /or combination of these. Due to the increase in modern wireless communication systems, tunable antennas are emerging for the better use of frequency spectrum [18]. Frequency tunable antennas are subset of tunable antenna in which frequency characteristics are tuned according to the tuning action. Frequency tunable antennas will enhance the functionality by providing the wireless terminals or handset with more frequency bands and bandwidth, maintaining the compact size and reducing the interference [19].

Based on the mode of operation frequency tunable antenna can be divided into continuous tunable antenna discrete tunable antenna. Tunable antennas yield compact sizes and improve significantly the data transmission efficiency [20]. Accordingly, a single tunable antenna with a wide tuning range would enable radio manufacturers to reduce costs by using a single frequency-agile device instead of a series of fixed frequency antennas [21]. Frequency agility is the capability of the antenna structure to

modify its frequency characteristics controlled and reversible manner [22]. This can be achieved by different methods either based on the physical alteration of the antenna structure, or by the use of smart materials like ferrites and liquid crystals in antenna or by incorporating a smart tunable element within the structure that enables the redistribution of surface currents [23]. In addition to that, the impedance and phase relationships intentionally modified within the structure after the tuning action [24].

As discussed, based on the tuning action tunable antenna can also be classified into integrating smart devices, physically tunable or material change. Either electrically tunable or optically tunable components can be embedded in to antenna structure. Frequency tunable antenna classification is summarized in Figure 9.

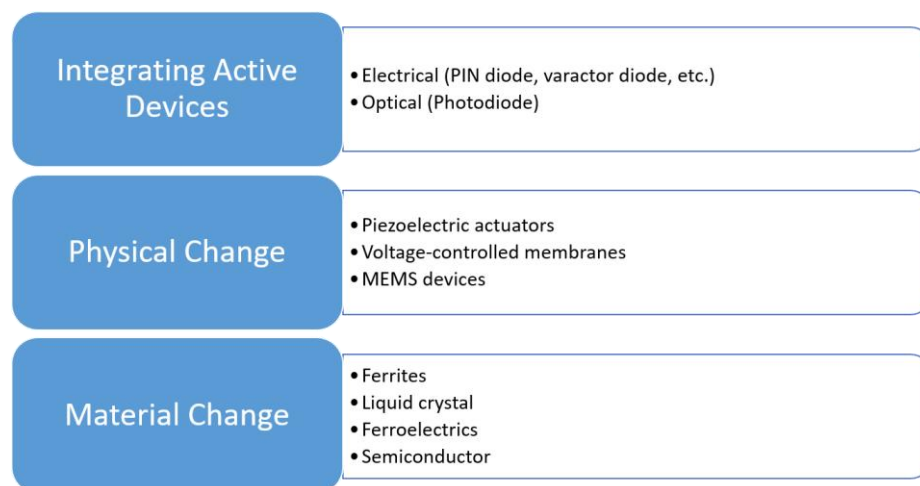


Figure 9: Frequency tuning techniques

Tunable antenna can be utilized to overcome the technology tolerances of the fabrication process, within which the tuning action is applied to fine-tuning the frequency characteristic to the desired setting [25]. Furthermore, they can be utilized in adaptive tuning, within which the antenna characteristics continuously can be adjusted due to any change in its environment [26]. Moreover, tunable antennas are

used to allow wireless terminals handset to select a specific service by adjust its frequency characteristics to the desired frequency band [27].

2.2.1 Electrically Tunable Antenna

In this context, several electrical tuning mechanisms and concepts have been intensively investigated; including Positive - Intrinsic – Negative (PIN) diode [28-32], varactor diode [20, 33-52], Schottky diode [53], Field-effect transistor (FET) switch [54], and radio frequency microelectromechanical systems (RF MEMS) based capacitors [55-59]. It is noticeable that the best tuning action for frequency tuning is with the application of a DC bias voltage that force the tuning component to either change its value as in the case of variable dielectric or semiconductor varactor [41]; or to change its position as in the case of MEMS [57]. It is always preferable whenever it is applicable, not to have both DC bias and RF signals exist simultaneously on the metallization pad [60]. Nevertheless, this not always the case, hence to avoid the detrimental effect on both the DC and RF sources, a bias tee or DC blocking capacitor may be needed to be used at the input feed [35].

All of these technologies have benefits and drawbacks in terms of power consumption, speed, reliability, microwave losses or drive voltage levels [22]. Therefore, a key factor in designing tunable antennas is the technology used for realizing the tunability. PIN diode is one of the switching electronic components used in the RF system to achieve tunability by altering the current distribution [28]. PIN diodes are a semiconductor device constructed by sandwiching an intrinsic semiconductor between positive and negative made out of silicon or GaAs. It can be modeled as a variable resistor at RF and microwave frequencies controlled by dc current [61]. They operate in two modes: on state mode where the diode is forward

biased and the off-state mode where the diode is not biased [30]. Moreover, a varactor diode is a voltage-controlled device in contrast to a PIN diode, which is a current-controlled, and it works only in reverse bias [61]. The capacitance of the varactor diode is varied by controlling the reverse voltage, so it works as a variable capacitor, within which the capacitance decreases by increasing the reverse bias [61].

On the other hand, RF-MEMS switch is based on altering the surface current path by using mechanical movement to achieve open or short circuit [55]. Electrostatic force produced as a sequence of the applied dc bias voltage between the movable membrane and the ground plane [57]. In MEMS based varactor; due to the electrostatic force, the movable membrane is pulled towards the actuation pad, which decreases the air gap and increases the total effective permittivity resulted in a downhill shift for the resonant frequency [59].

A state of art of various type of tunable antennas with different tuning techniques have been described in this section. Upadhyay et al. has introduced a multiband reconfigurable antenna for ITS applications with total length of 29.6 mm and width of 26 mm on FR-4 epoxy substrate [28]. A PIN diode is used to operate the structure at different frequencies without changing in the antenna size. In the on state of the diode, the antenna resonates at the frequency bands 1.25-1.5 GHz, 1.88-2.1 GHz, 2.77 – 3 GHz and 5.675 – 3.79 GHz. Meanwhile in the off state, the antenna resonates at frequency bands 1.52-1.6 GHz, 2.1-2.22 GHz, 2.75-3 GHz, 3.82-4 GHz, and 4.25-4.65 GHz.

Tong Li et al. proposed a frequency-reconfigurable bow-tie antenna by integrating over the arm. The bow-tie radiator is printed on both sides of the substrate and is driven by a microstripline that is followed by two parallel strips. Antenna

operates in different frequency bands 2.2–2.53 GHz, 2.97–3.71 GHz, or 4.51–6 GHz band [29].

Symeon et al. developed a pin diode loaded frequency and pattern tunable annular slot antenna which operates in 5.2, 5.8 and 6.4 GHz frequency bands. Two MBP-1035-E28 PIN diodes are integrated in the design. When forward biased, each diode acts like a short, and when reverse biased, it behaves like a capacitive load. When no diodes are forward biased in the above situation, the slot antenna acts like an unloaded one [30].

Chattha et al. designed a frequency reconfigurable patch antenna with pin diode along with bias tee. Proposed antenna is switchable between 2.4, 3.6, 4.9, 5.1, and 5.9 GHz. Two BAR 64 PIN diode were integrated in the antenna system to act as the tuning element between 3 metal patches [32].

Anagnostou et al. introduced a coplanar reconfigurable folded slot antenna incorporating pin diode. Two frequency bands 5.1 and 5.75 GHz and are covered in this design by using pin diodes to bind and disconnect the metallic strips from the ground plane. The pin diodes are biased from the back side of the substrate through vias [31].

Yoon et al. designed a reconfigurable antenna using varactor diode for LTE application in the range between 690-804 MHz and 1704-2268 MHz [33]. The antenna exhibits a gain between -1.97 to -0.43 dBi and a radiation efficiency 3.33-43.77% over low and high bands over the whole tuning range. Hum et al. has proposed a differentially fed frequency agile patch antenna by integrating set of varactor diodes for achieving a frequency tuning from 1.8-3.2 GHz [34]. The antenna was designed

using Rogers RO3203 substrates with a physical dimension $L=32$ mm, $w=9$ mm, $h_1=1.524$ mm (first layer's thickness) and $h_2=0.813$ mm (second layer's thickness). Huitema et al. incorporates both a magneto–dielectric material and a varactor diode for achieving ultra-compact size and tuning over DVB-H band from 470-862 MHz [35].

Pujari et al. has introduced a circular microstrip patch antenna and tuned using varactor diodes for X band communication [36]. Furthermore, Zhang et al. has developed a rectangular microstrip antenna for L band on Rogers RT/duroid5880 substrate ($\epsilon=2.2$, and substrate height $h=1.6$ mm) and the dimension $L=5$ cm, $W=8$ cm [37]. Eight varactor diodes were loaded at the two radiating edges for the structure, the resonant frequency was changed from 1.45-1.8 GHz by changing the reverse bias voltage 0.2-20V and return loss less than -12dB along with the tuning range. Deo et al. has demonstrated a patch antenna of two L slots and a U slot in the ground plane with dimension $L=27$ mm, $w=25$ mm [38]. Three varactor diodes are inserted in these slots for tuning the operating frequency, which configured as RLC lumped elements for three different states. Khelladi et al. has proposed a narrowband frequency microstrip tunable antenna with a rectangular shaped slot [39]. A variable capacitor is placed on the slot for achieving tunability from 2.2-2.6 GHz due to change of the capacitor value from 7.5pF to 4pF. Meng et al. has designed a fork shaped wideband microstrip patch antenna tuned using four SMV2020 varactors [40]. The measured frequency agility is 24% from 1.47 GHz to 1.84 GHz by changing the reverse voltage of diodes from 0 to 20 V. Malcolm et al. has reported a reconfigurable planar Inverted-F antenna loaded using varactor diodes [41]. The capacitance changes from 19 pF to 1.5 pF by changing the biasing of varactor from 0 to 23 V and the structure shows a possible effective bandwidth of 56%.

Boukarkar et al. has proposed a compact dual-band frequency tunable antenna for WIMAX and WLAN applications [42]. The resonant frequency was tuned by integrated two varactor diodes from Infineon BB85. Two bands have been tuned continuously and covered the WIMAX band (3.28-3.51 GHz) and WLAN band (5.47-6.03 GHz). Behdad et al. has designed a varactor based dual-band slot antenna by loaded it in a proper position [43]. The capacitance range was tuned from 0.5-2.2 pF, which achieved a frequency tuning from 1.2 to 1.65 GHz by increasing the dc biasing voltage from 1.5 to 30 V. Elfergani et al. has loaded a varactor at the top of printed dual-band monopole structure consists of a hexagonal patch and defected ground plane [20]. The lower band shifted from 3.2 to 5.1 GHz, while the upper band shifted from 7.25 to 9.9 GHz.

Khidre et al. proposed a patch antenna with a varactor loaded slot for reconfigurable dual band operation [44]. Antenna consist of a variable capacitor in the middle of a slot and resulted in two resonant frequencies. First resonant frequency changes from 2.22 to 2.26 GHz, while the second resonant frequency changes from 3.24 to 4.35 GHz by varying the DC supply to 30 V.

Holland et al. developed tunable coplanar patch antenna using varactor as tuning element [45]. The coplanar patch antenna exhibits frequency tunability from 4.92 GHz to 5.40 GHz corresponds to the change in DC supply from 0 to 19.5 V. Garcia et al. proposed a frequency agile phase-conjugating active antenna with a slot located closer to one of the radiating edges [46] The antenna consists of a varactor diode located on the radiating edge opposite to the slot. The antenna exhibits frequency shifts from 770 to 870 MHz by changing DC bias voltage 3.5 V to 30 V. Turk et al. developed a CPW-FED frequency-agile shorted patch using varactor diode [47].

Microstrip patch is connected to the signal trace of the CPW line via varactor placed near the radiating edge. Frequency characteristics shifts from 4.26 to 4.58 GHz by changing DC voltage from 0 to 25 V. Madi et al. designed a frequency tunable cedar-shaped antenna for WIFI and WiMAX applications using 6 varactors and 1 pin diode [48]. Proposed antenna achieves wide tunability in a 1.45 GHz and 4.6 GHz when 3 pairs of varactors are connected across slots. Additional pin diodes achieve reconfigurability in the dual band between 2.5 and 4 GHz and a single band of 6.6 GHz.

Sondaş et al. has suggested a loop-loaded printed dipole antenna for dual-band (3/5.2 GHz) [49]. The proposed dipole is located between a pair of rectangular loops supported by a Rogers RT/duriod 5880) substrate with a thickness $h=0.75$ mm and $\epsilon=2.2$. A single band 3 or 5.2 GHz has been tuned and achieved with bandwidth 23% and 17%. Bai et al. has proposed an L shape patch with three slots in the ground plane fed by one microstrip line for tri-band antenna design [50]. Three operating bands was supported over the frequency 0.6-1.1 GHz, 1-2.5 GHz and 1.9-2.7 GHz by using three digital tunable capacitors. Mansour et al. proposed a continuously tunable wimax band, notched UWB antenna with fixed WLAN notched band. The antenna uses a novel miniaturized resonator and capacitors tuned between 0.1 pF to 0.2 pF to achieve the required tunability within the range of 3 GHz to 4 GHz [51]. Mansour et al. designed a switchable planar monopole antenna between ultra-wide band and narrow band behavior [52]. Antenna operates at WLAN frequency band or switchable in UWB for capacitor value of 0.1 pF and 0.8 pF respectively.

Haskins et al. developed a Schottky diode based tunable antenna. Antenna achieves tenability from 2.19 GHz to 2.28 GHz with the application bias voltage

between 0 and 30V. Schottky diode is placed in a position to ensure maximum tuning range. Radiation pattern is well preserved in the tuning range; however, these types of antenna suffers from increased losses [53].

Kawasaki et al. designed a FET based frequency tunable slot antenna [54]. When the gate voltage is between 0 and pinch off voltage, loading impedance of the transistor is utilized to shift frequency characterizes by changing the length of the slot. Antenna Achieves frequency tenability from 9.22-10.22 GHz by adjusting the gate to source between 0-0.6 V.

Wright et al. proposed a MEMS based tunable broadband patch antenna for conformal applications [55] The designed tunable antenna has three reconfiguration states that allowing the frequency characteristics to shift between 1.13 to 1.7 GHz. Saha et al. has represented a tunable patch antenna loaded with a split ring resonator and embedding four RF MEMS as tuning element [56]. The tunability is achieved by changing the capacitive gap of the switch between up and down state with gap 1.5 μm and 1 μm , respectively. Antenna provided 0.28 GHz, 1.6 GHz, 0.4 GHz and 1.97 GHz frequency bands of operation when antenna is loaded with one, two, three and four switches respectively. The activation voltage is 10.4 V.

Erdil et al. designed frequency reconfigurable microstrip patch antenna using RF MEMS as tuning element. Reconcilability is achieved by loading the patch with a coplanar waveguide stub on which variable MEMS capacitors are mounted [57]. As the actuation voltage is raised from 0 to 11.9 V, the resonant frequency can be continuously varied from 16.05 GHz to 15.75 GHz.

Similarly, Barrio et al. introduced a miniaturized antenna incorporating MEMS tunable capacitors [58]. The antenna volume has been decreased using a tunable component with efficiency above 50% and tuned frequency from 700-930 MHz. Jackson et al. demonstrated a tunable circular microstrip patch antenna assisted by RF MEMS [59]. The proposed antenna operates between 16.91 GHz to 16.64 GHz with the application of 0 V to 165 V. The electrostatic force of attraction caused by the applied dc bias voltage causes the movable patch to deflect downward toward the fixed ground plane.

Table 2: Comparison of electrically tunable methods

Feature	PIN diode	FET	MEMS	Varactor diode
Bias Voltage	Low	Less than 5V	Need High activation voltage	High
Insertion Loss	Low	Low	Low	Moderate
Tuning Mode	Discrete	Discrete, Continuous	Discrete	Continuous
DC Power Consumption	Moderate	Negligible	Low	Low
Cost	Inexpensive	Inexpensive	Expensive	Inexpensive
Bias Network	Complex	Moderate Complex	Needs Hermetic packaging	Complex
Power Handling capacity	Low to Moderate	Low to Moderate	Moderate	Moderate
Other Features	Fast Switching speed	Fast Switching speed	Lower Reliability	Easy to integrate

Based on the performances of the tunable antenna different electronic tuning methods are compared and summarized in the Table 2. All techniques differ in terms of power consumption, speed, reliability, microwave losses or drive voltage levels [22]. PIN diode based tunable antenna can give good performances with lower bias

voltage but application is limited for discrete tuning. Varactor based tunable antenna is widely employed for continued tuning due to ease of integration and good power handling capacity. The main issue with varactor diode based tunable antenna is, it requires high bias voltage normally above 20 V to achieve reasonable tunability.

Most of the tunable antenna design discussed in the literature either uses multiple varactor diodes as tuning elements or it has high larger size. Tunable antenna with compact size requires high bias voltage. The project mainly aimed the design of a tunable antenna within 1 to 2 GHz, because application such mobile services, aircraft surveillance, satellite navigation including global positioning system (GPS), global navigation satellite system (GLONASS), BeiDou, etc. uses L band. Design of a tunable antenna with following specification is still a challenge for researchers, and there is no reported work which satisfies all these specifications,

- Compact size
- Continues Tuning
- Single varactor diode
- 1 to 2 GHz frequency
- Lower bias voltage

The proposed work illustrates the design and testing of a compact single varactor tuned microstrip patch antenna design with lower bias voltage, which is the first component of RF front end part in Wireless antenna multiplexing system. The remaining tunable components in the RF front end like tunable band pass filter, tunable oscillator also employs voltage-controlled tuning, and each component has individual

biasing requirement for each frequency. In order to synchronize and control all these tunable devices a control unit is required. A PIC microcontroller-based control unit is also designed in the work.

Chapter 3: Wireless Multiplexing Agile Antenna-based Control System

Multiplexing and Multiple access technologies are becoming vital components for high-performance wireless communication system. Whereas multiplexing techniques employing either multiple antennas or multiband/wideband antennas for multiplexing are commonly used, these techniques have inherent drawbacks. A feasible solution to this is to employ frequency reconfigurable or frequency agile antennas. This approach has advantages from both multiple antenna and multiband/wideband antenna designs. In this paper, a hardware implementation of a proposed biasing and control circuit/system for wireless multiplexing that utilizes a frequency reconfigurable or frequency agile antenna is reported. The device comprises a microcontroller, DAC, CMOS oscillator, power module and a USB interface for communication with a custom-built software installed on a PC. The device has functions for control, digital signal processing and de-multiplexing. The device is fed with an input multiplexed signal, and the de-multiplexed output signals are extracted and displayed on the graphical user interface of the software [62]. Due to the re-configurability and programmability of the device, it presents a flexible, cost effective solution for a variety of real-world applications.

3.1 Proposed Solution

A basic circuit/system architecture for wireless multiplexing using tunable antenna is shown in Figure 10. The tunable antenna collects signals from a single or multiple surrounding antenna. A matching circuit is required to minimize the mismatch between the antenna intrinsic input impedance and the impedance of the Tunable band

pass filter (BPF) which is the next stage of the wireless multiplexing system. The BPF is need to filter out other harmonics and to minimize interference signals.

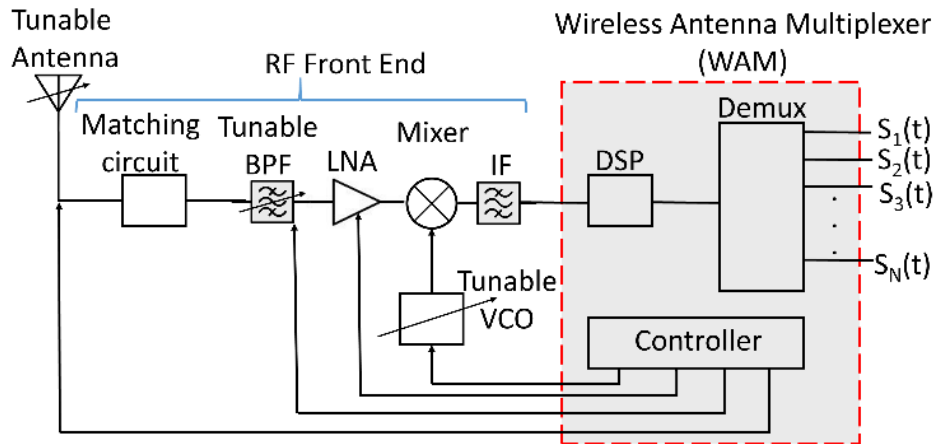


Figure 10: Wireless antenna multiplexing system

The signal is then fed to the Low Noise Amplifier (LNA), that amplifies a very low-power signal without significantly degrading its signal-to-noise ratio. The received signal is then down-converted to recover the modulated baseband signal through the help of a tunable oscillator. The tunable antenna, filter and oscillator are all controlled by a control unit, which is responsible for synchronizing and setting all of them to the same frequency. The output signal after the multiplexing process is then processed depend on the modulation protocol. The original data can then be separated and extracted from the baseband signal using a de-multiplexing unit.

3.2 Biasing Overview

Consider a system where the tunable multiplexer needs to listen to four different frequencies f_0 to f_3 . For each frequency, the tunable devices of the system have individual biasing requirements. The control unit establishes a system for

selection of the required bias voltages for each frequency, for each device. Consider also, two approaches to achieving this. The first method utilizes a quantized, rectified sinusoidal wave as shown in Figure 11.a. This is generated by passing sinusoidal wave through an Analog to Digital Converter (ADC). The resultant signal has the same shape as sinusoid but with step levels. The signal is then rectified to make all the steps positive. The second method utilizes a quantized saw tooth waveform as depicted in Figure 11.b, which is generated by passing a saw tooth waveform through an ADC. Each step of the quantized waveforms represents a different DC voltage bias level corresponding to a particular frequency selection. For example, with bias voltage V_0 , frequency f_0 is selected, for bias voltage V_1 , frequency f_1 is selected and so on.

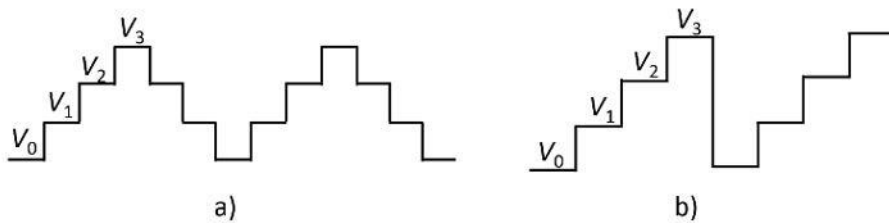


Figure 11: Quantized waveform (a) rectified sinusoidal wave (b) saw tooth wave

The two approaches treat frequency selection differently. With the first approach, as the voltage increases, the frequencies are selected in order, then as the voltage decreases, the frequencies are selected in reverse order as shown in (1).

$$f_0 \rightarrow f_1 \rightarrow f_2 \rightarrow f_3 \rightarrow f_2 \rightarrow f_1 \rightarrow f_0 \quad (1)$$

With the second approach as the voltage increases, the frequencies are selected in order then the selection loops back to start from the first frequency as shown in (2).

$$f_0 \rightarrow f_1 \rightarrow f_2 \rightarrow f_3 \rightarrow f_0 \rightarrow f_1 \rightarrow f_2 \rightarrow f_3 \quad (2)$$

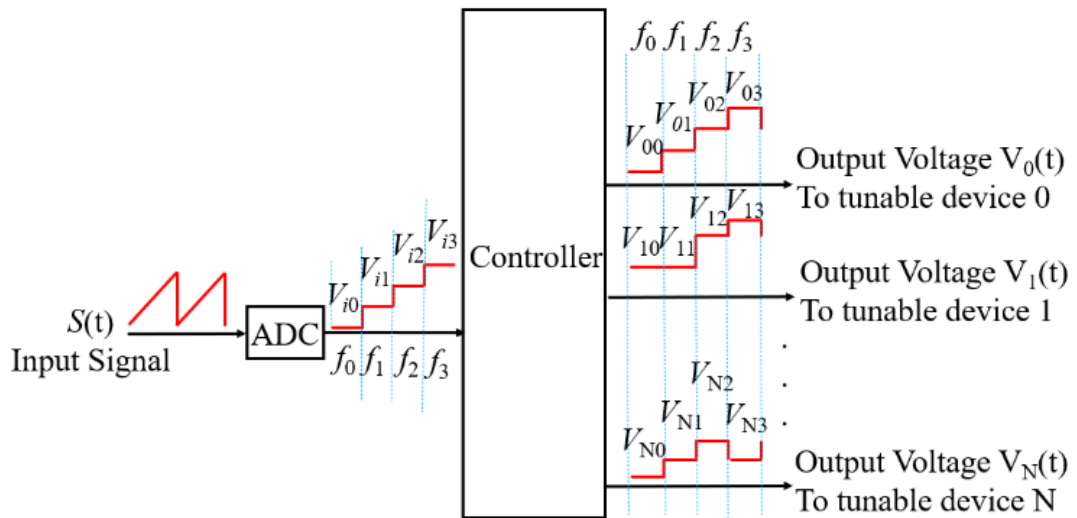


Figure 12: Multiple device biasing

The steps described above provide biasing voltage for a single device, however the tunable multiplexer has several tunable devices that require synchronized biasing for the system to operate at a particular frequency. The controller provides for this as illustrated in Figure 12. It makes available the necessary bias voltages required for operation of the respective tunable devices at the desired frequency, depending on the input signal.

3.3 Wireless Antenna Multiplexer (WAM) Unit Blocks

The fabricated WAM board is shown in Figure 13 and the main components are explained below.

3.3.1 PIC

A 32-bit PIC microcontroller (PIC32MK1024GPD064), from Microchip [63] is used as the main controller of the board. It features 7x 12-Bit ADC's, each operating

at up to 3.75 MSPS, which can be combined and sequenced to provide up to 18 MSPS sampling rates.

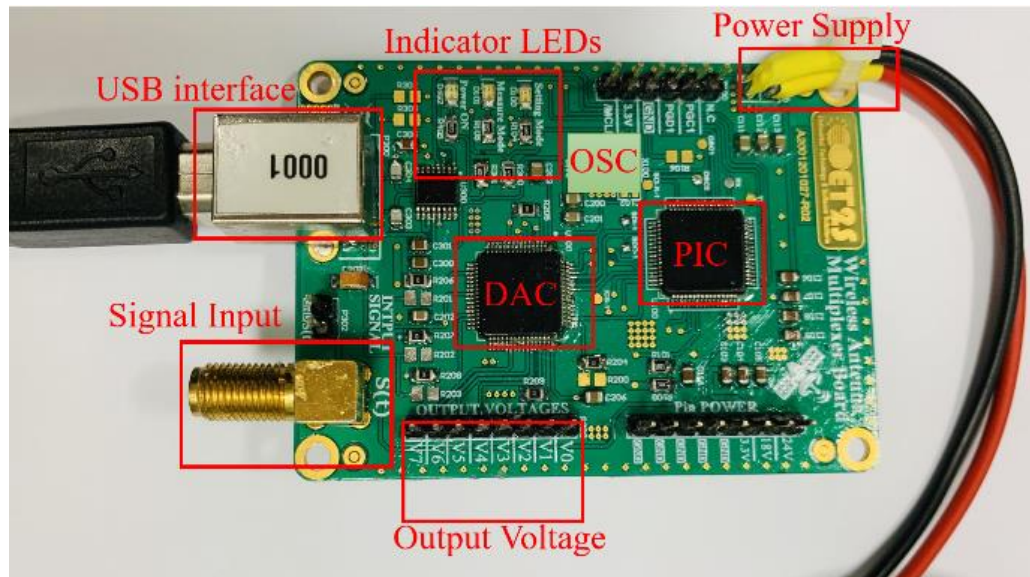


Figure 13: Wireless Antenna Multiplexing (WAM) board

3.3.2 Digital to Analog Converter (DAC)

A 12-bit, Serial Input Digital to Analog Converter (DAC7718) from Texas Instruments [64]. This is a low power, ± 16.5 V output converter with eight DAC channels.

3.3.3 Universal Serial Bus (USB) Interface

USB to asynchronous serial data (UART) interface, allowing the microcontroller-based designs to communicate with the personal computer using a virtual COM port.

3.3.4 Oscillator

The microcontroller internal timing is generated with input from the 12 MHz oscillator unit. It is an XO (standard) Complementary metal oxide semiconductor (CMOS) Oscillator from Kyocera [65] (KC2520B12.0000C10E00).

3.3.5 Power Module

This consists of the input power supply of 24 V and 2 DC/DC buck (step-down) regulators. The first is a LMR14006 is a PWM DC/DC step down regulator from Texas Instruments. This is used to step down the voltage from 24 V to 18 V, 500 mA in the WAM board. The device has built-in protection features such as pulse-by-pulse current limit, thermal sensing and shutdown due to excessive power dissipation. It provides up to 18 V for output port biasing. The second DC/DC buck (step-down) regulator is the TPS5410 high output current PWM DC/DC step down regulator from Texas Instruments. This is used to step down the voltage from 24 V to 3.3 V, 1 A in the WAM board. It provides power for the PIC microcontroller, oscillator, DAC and USB interface. The power module ensures that three voltage levels, 24 V, 18 V and 3.3 V are available on the board.

3.3.6 WAM Application

This is a customized application built for programming and running the WAM system board. It also provides the controller function. The application has three modes, PROGRAM, RUN and OFF mode.

3.3.7 Indicator LEDs

The device has three LEDs labelled “Power ON”, “Settings Mode” and “Measure Mode” to indicate when the device is powered, when it is being programmed and when it is in the run mode respectively

3.3.8 Input Ports

It has two input ports. One is header pin, which allows for wire connection. Other port allows for connection via SMA. The ports allow for input voltages of 0 V to 3.3 V.

3.3.9 Output Ports

The output voltages are taken from the V_0 to V_5 pins. Port V_6 is an unused port for redundancy. The pins output voltage is in the range of 0 V to 18 V. Port V_7 provides a triangular, test signal output voltage of 0 V to 3.3 V.

3.4 Device Operation

The block diagram illustrating the device operation is shown in Figure 14. The input to the programmable WAM System board at either input port is an analog signal $S(t)$. The internal ADC of the microcontroller samples the input signals every 3.2 ms, and sends it to the desktop application through a byte sequence.

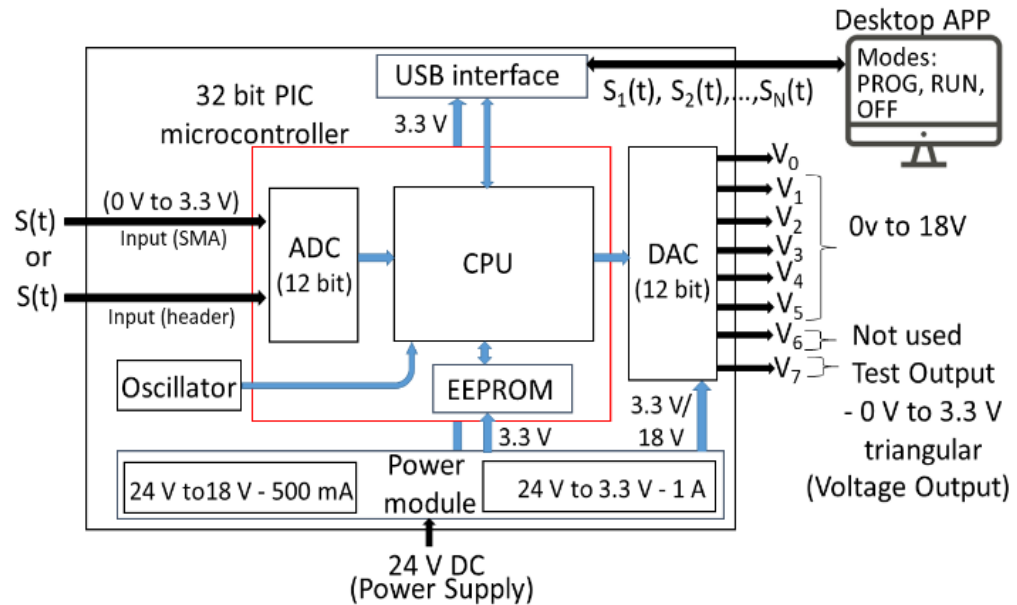


Figure 14: WAM system board operational block diagram

The byte sequence includes 4 bits containing the Step ID (a value assigned to a set of sample points received for a specified frequency), 12 bits containing the digital value of the measured signal $S(t)$ and 8 bits containing the end of frame delimiter. The information is sent via the USB interface that creates a virtual COM port for communication with the application on the PC. The WAM application allows for data display and device programming. The configuration settings for the DAC can be programmed in the “Settings” tab. For each Step, the DC voltage bias level (mV) for each of the output voltages at ports V_0 to V_5 , as well as the duration (μs) these voltage levels should be held is specified. This information can be saved in the internal EEPROM memory of the microcontroller.

For system biasing, the software initiates an infinite loop. For each Step, the 12-bit digital value is sent to the DAC via the microcontroller using the SPI connection. Basing on the configuration setting, the output voltage at each of the

output ports (V0 to V7) is maintained for the specified duration, which should be long enough for device synchronization. At the expiry of this duration, the digital value for the next Step is sent from the application to the DAC, and the process repeats. As the voltage bias levels change, the frequency of operation of the wireless antenna multiplexing system correspondingly changes and the device is able to receive information from various external antennas working at different frequencies. Through this process, the de-multiplexed input signal data is made available sequentially in the WAM application. It can be viewed in the “Graph S (t)” tab and the data can be extracted from the “Data” tab for further processing in MATLAB or any other application as required.

3.5 Measurement Setup

The measurement setup for testing is illustrated in Figure 15. The WAM board is supplied with 24 V DC as shown in Figure 16. The test output signal from pin V7 was connected to provide a triangular signal test input voltage $S(t)$ at the header pin input port. $S(t)$ is a multiplexed signal defined by (3).

$$S(t) = \sum_{i=0}^7 s(t)Step(i) \quad (3)$$

Where i is the step number, and $s(t)Step(i)$ is a demultiplexed signal that corresponds to step number i . A USB connection was made between the device and a laptop on which the WAM application was hosted. The voltage at the output ports were measured by connecting the output pins to an oscilloscope.

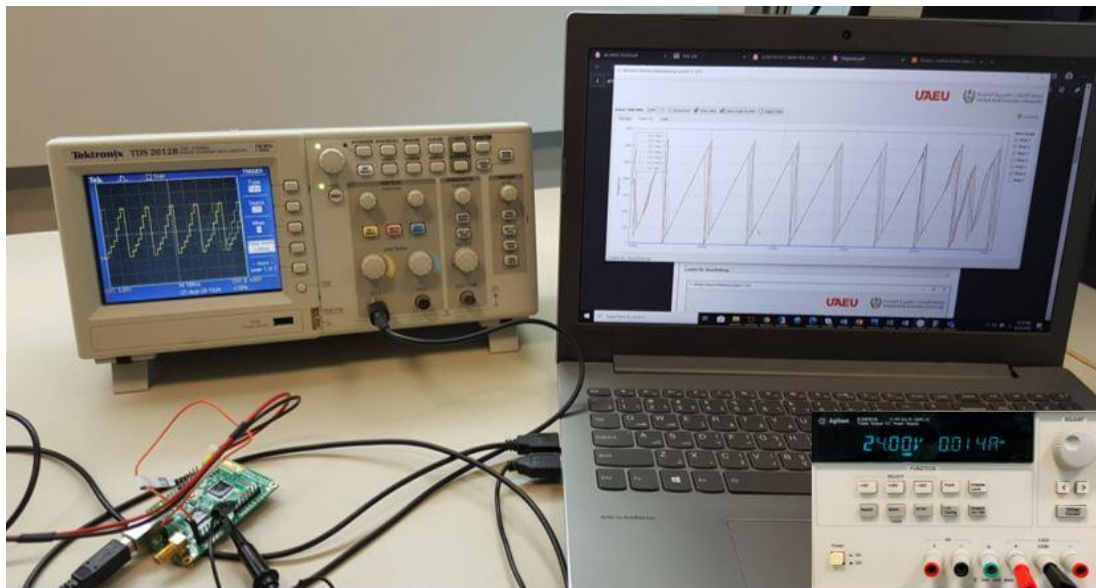


Figure 15: Measurement Setup



Figure 16: DC power supply to the board

3.6 Results and Discussion

The real time plot of the de-multiplexed signals are displayed in the application is shown in Figure 17. The x-axis represents number of samples and the y-axis represents voltage in mV. The signal has a maximum voltage of about 3.3 V. The device is hardwired to measure up to seven steps. Each Step is color coded. The

application allows for individual display of the Steps or simultaneous display of all Steps.

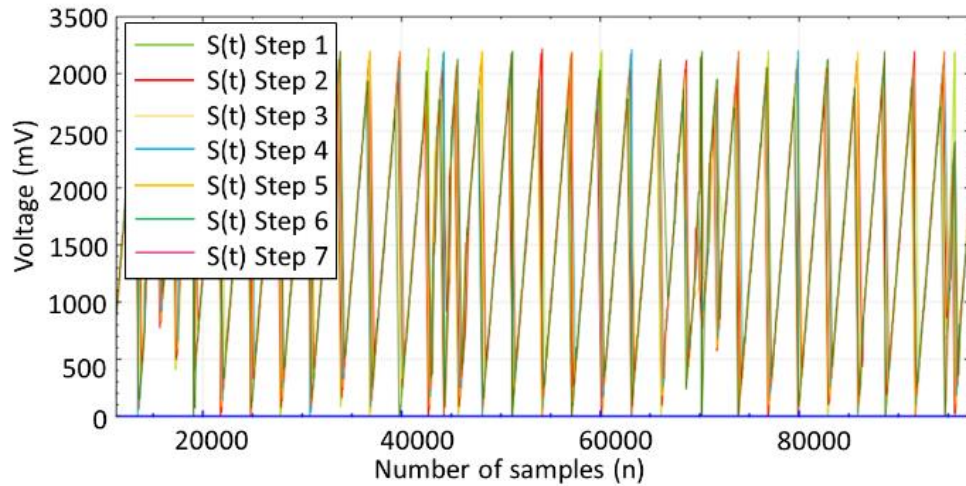


Figure 17: Plot of de-multiplexed input signal $S(t)$ in the WAM application

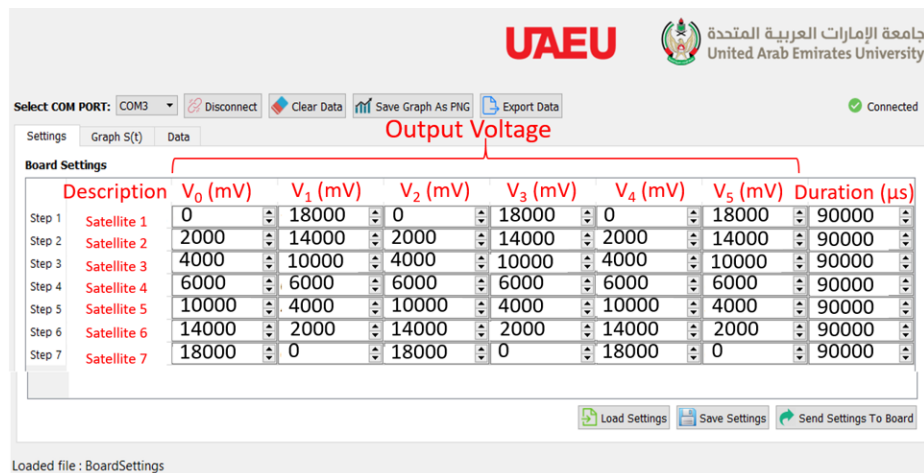


Figure 18: Board configuration settings

The board configuration settings are illustrated in Figure 18. Each row represents a Step. For each step the bias voltage level at output port V_0 to V_5 is

specified along with the duration. For example, as illustrated in the figure, for Step 1, the voltage at ports V_0 to V_5 , alternates between 0 V and 18 V.

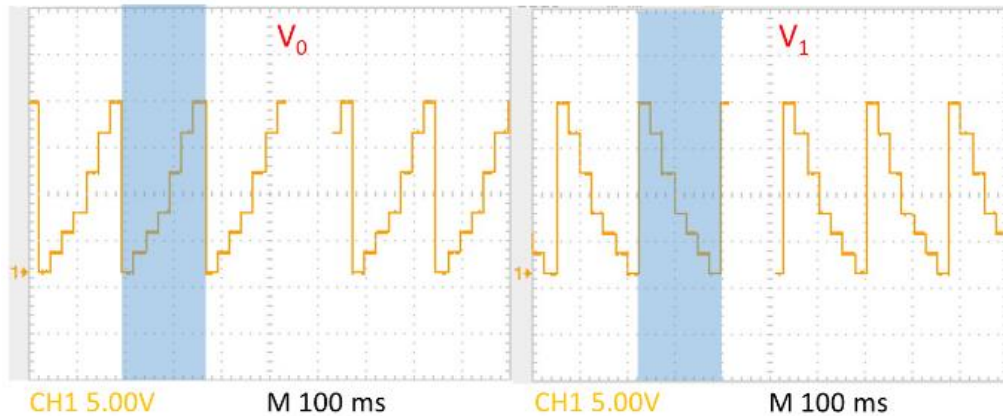


Figure 19: Voltages at pins V_0 and V_1 measured using an oscilloscope

These voltages are maintained at their respective values for 90 ms. At the end of this period, Step 2 output voltages are then output. This screen also contains options for programming the board, saving settings, and loading previously saved settings. The output voltages extracted using the oscilloscope for pins V_0 and V_1 are shown in Figure 19. The shaded areas highlight corresponding time intervals. As the voltage at V_0 increases from 0 V, 2 V, 4 V, 6 V, 10 V, 14 V and 18 V, the voltage at V_1 decreases from 18 V, 14 V, 10 V, 6 V, 4 V, 2 V to 0 V. The horizontal levels correspond to the 90 ms that the biasing levels are held. It should be noted that DC-RF isolation techniques, such as through multilayer technology and guarding rings, would need to be considered for incorporating the RF front end.

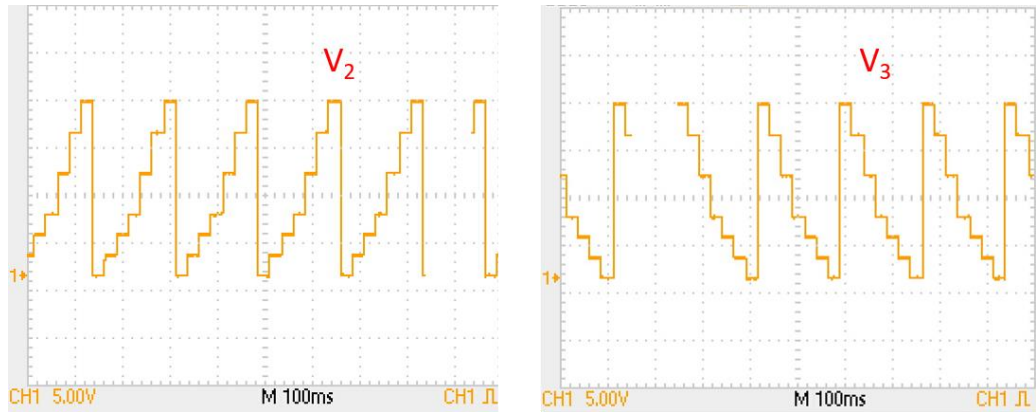


Figure 20: Voltages at pins V_2 and V_3 measured using an oscilloscope

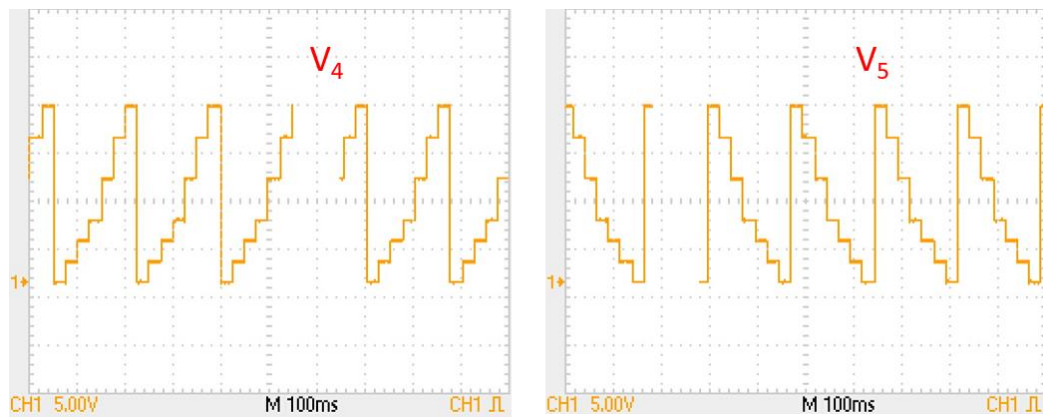


Figure 21: Voltages at pins V_4 and V_5 measured using an oscilloscope

Remaining output voltages taken from oscilloscope for pins V_2 to V_5 are shown in Figure 20 and Figure 21. All the voltage levels are either increasing or decreasing between 0 to 18 V. User can program the voltage levels to any value between 0 to 18 V in the board configuration settings and these changes can be applied instantaneously to the WAM board without any delay. The main feature of the proposed WAM control board is the reconfigurability and instantaneous response. The developed WAM control system can collect signals from seven satellites and which can be further increased by reprogramming the module.

Chapter 4: Compact Frequency Reconfigurable Microstrip Patch Antenna

4.1 Proposed Design Overview

A novel single varactor frequency reconfigurable microstrip patch antenna is presented in this project. The antenna comprises a novel symmetrical arrangement of four patch metallisation coupled and interconnected to each other via slots and metallic bars respectively. The antenna structure is excited through a single feed probe connected to one of the patches. To achieve a compact size of 22 mm x 21 mm x 1.57 mm, a shorting pin is placed close to the feed point which pulls down the antenna's resonant frequency. By adding a varactor diode at the centre of the patch, frequency re-configurability is introduced. Variation of the varactor DC reverse bias voltage from 0 V to 7.5 V results in a corresponding resonant frequency shift from 1000 MHz to 1150 MHz, giving a tuning range of 15%. The proposed design is compact and achieves frequency reconfiguration, with a single varactor diode and a low bias voltage requirement as compared to reported works. The antenna can find application in various existing and emerging communication systems.

4.2 Frequency Reconfigurable Antenna Design and Simulation

The development of the reconfigurable antenna is illustrated in Figure 22. The design began with a square patch with truncated corners (Antenna 1). Next slots were etched into the four sides of the antenna (Antenna 2). The slots introduce an inductance. This is due to the lengthening of the current path as the current is forced to meander around the slots towards the radiating edges. This inductance causes a drop in the resonant frequency from 3.05 GHz to 2.41 GHz as shown in Figure 23. To allow for insertion of the varactor diode at the center of the patch for symmetrical behavior,

the antenna was split into two by means of a horizontal 1 mm slot (Antenna 3). The current path is cut off and this results in a capacitive effect across the center of the patch, resulting in a reduction of the resonant frequency to 2.04 GHz. To facilitate further miniaturization, a pin was inserted close to the feed position (Antenna 4). This pulled down the resonant frequency of the antenna from 2.04 GHz to 1.21 GHz as shown in Figure 23. The pin also improved the return loss by providing a shunt inductance close to the probe feed which improves impedance matching by driving input impedance closer to the 50 Ω design input impedance [66]. Lastly a varactor diode was added at the center of the patch to introduce frequency reconfigurability (Antenna 5). The addition of the varactor introduces a capacitance which reduces the resonant frequency of the antenna further but degrades the impedance matching. The varactor can however be used to manipulate the coupling impedance and phase relationships between the upper and lower halves of the patch by changing its capacitance with the application of a DC bias voltage [24].

It should be noted that an antenna resonant at the same frequency as antenna 5, designed on the same substrate without any miniaturization, has a patch size of about 76 x 60 mm [67]. Thus, the proposed design provides miniaturization of about 90%. Basic transmission line theory and antenna design principles are used to develop final structure. Generally, the resonant frequency of a patch depends on its resonant length, which is longer than its physical length due to the fringing effect. This is where fringing fields that causes radiation exist in both air and the substrate and give rise to an effective dielectric constant and make the patch electrically larger compared to its actual physical dimensions. This suggests that to achieve miniaturization, as the physical dimensions are reduced, the extension length (due to the fringing fields) would have to increase, hence a miniaturized patch would have larger fringing fields.

The details final design is shown in Figure 24 and the structure is divided by two sections, section 1 and section 2. The proposed antenna's structure consists of four-coupled patch metallization labelled P1 to P4. The geometrical dimensions of proposed antenna are ($L = 10$ mm, $W = 9$ mm, $LC = 1.414$ mm, $SH = 3$ mm, $SW = 1.5$ mm, $SL = 7$ mm, $SSV = 1$ mm and $SV = 2$ mm. $PW = 9$ mm, probe $PL = 5.03$ mm, $PPW = 11$ mm, $GL = GW = 25$ mm). The antenna is excited by a coaxial probe located in the P3 metallization. The proposed antenna was designed using FR4 with a substrate of thickness 1.57 mm, dielectric constant of 4.4 and a loss tangent of 0.001 at 1 GHz. The antenna patch has a compact size of 22 mm x 21 mm x 1.57 mm and together with ground plane complete antenna structure has an overall size of 25 mm x 25 mm x 1.57 mm.

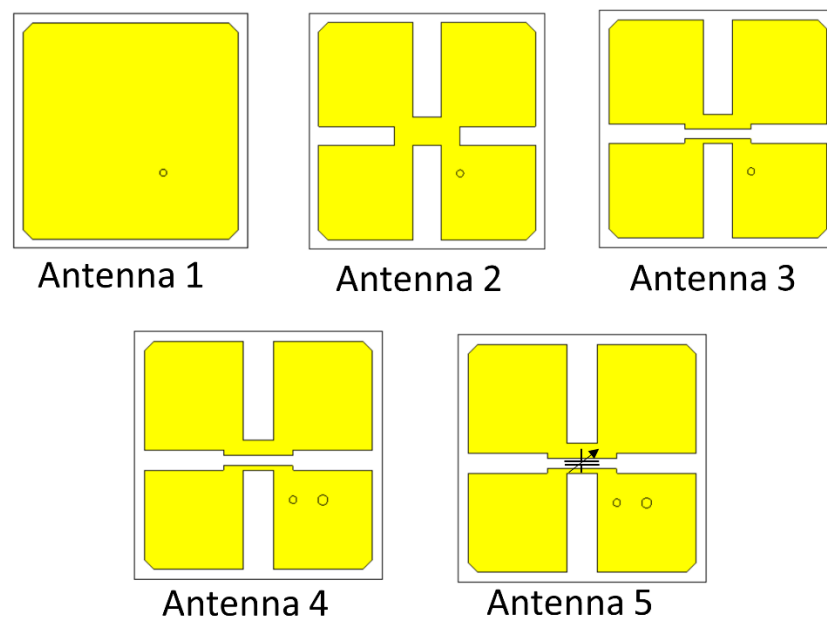


Figure 22: Evolution of the reconfigurable antenna design

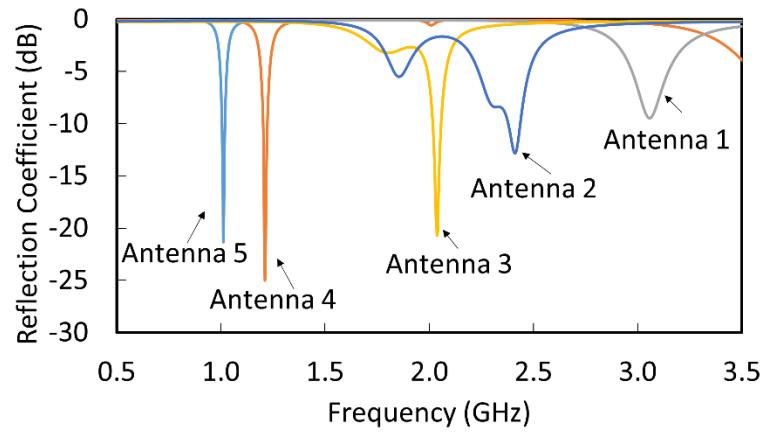


Figure 23: Return loss and resonant frequency shift with antenna evolution simulation results from CST

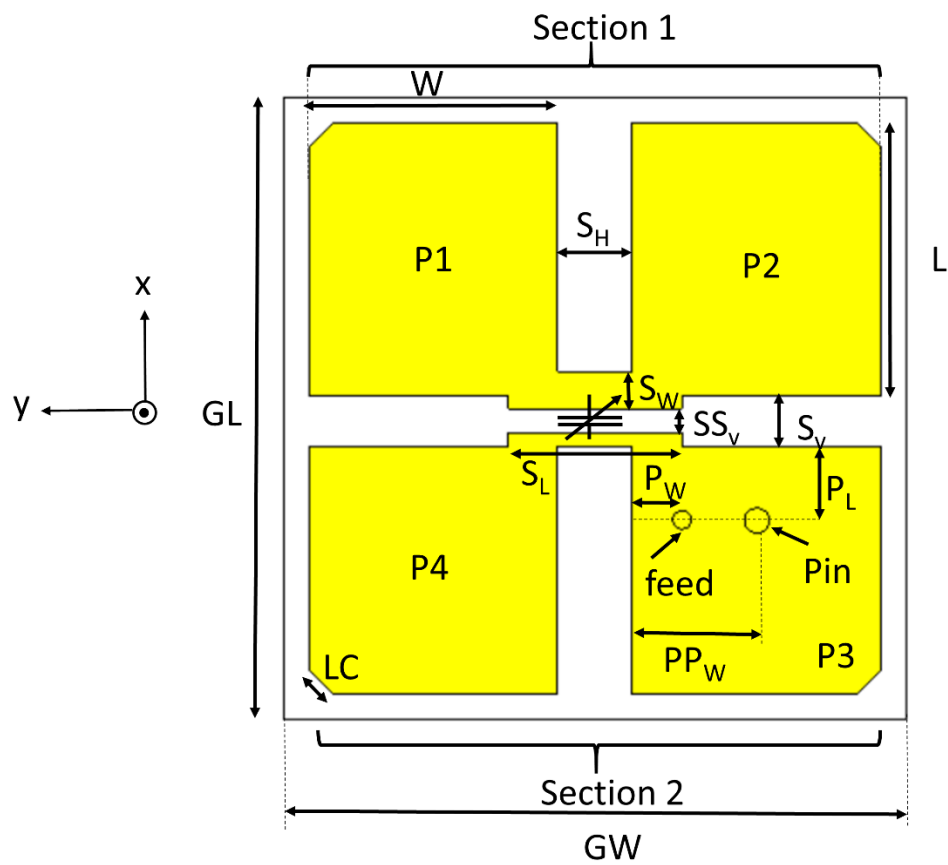


Figure 24: Antenna structure with dimensions

The SMV1234 varactor was used as the tuning element. Its equivalent spice model is shown in Figure 25 with L is the self-inductance with a value of 0.7 nH, R represents the DC losses with a value of 0.8 Ω . C counts for the tuned capacitance values versus applied DC Bias at 500 MHz as shown in Figure 24. The corresponding capacitance voltage dependency of the SMV 1234 are presented in Figure 26.

By applying DC bias, the capacitance of the varactor changes from 9.63 pF with the application of 0 V to 1.72 pF with the application of 7.5 V. The simulated effect of different bias voltages on the antenna resonant frequency is shown in Figure 27. At zero-bias, the antenna has its resonant frequency at 1010 MHz. As the applied bias is increased gradually, the capacitance decreases, pushing the antenna resonant frequency higher. For the highest bias voltage of 7.5 V, the antenna resonant frequency is shown to be 1160 MHz. The electromagnetic field distribution of the antenna for zero bias is illustrated in Figure 28, for the xy and xz planes. Changing the orientation of the central slot and varactor diode by 90° shows a similar trend in the resonant frequency shift, however with poorer return loss of not more than -14 dB except for the zero bias case due to impedance mismatch. Also, because this orientation puts the radiating edge long the shorter dimension the resonant frequencies are slightly higher.

The equivalent circuit of the antenna from transmission line theory is shown in Figure 29. Resistances RP_1 , RP_2 , RP_3 and RP_4 represent the radiation resistances and capacitances CP_1 , CP_2 , CP_3 and CP_4 represent the fringing effect at the radiating edges of the four-patch metallization P1, P2, P3 and P4 respectively. They can be determined by equations given in [68]. The inductances LP_1 , LP_2 , LP_3 and LP_4 account for the current detour around the slots. The shunt inductive effect of the pin near the feed is represented by LP_N . Capacitors C_{S1} and C_{S2} account for the capacitive effect

across the central gap. The varactor diode is modelled by the lumped variable capacitor C_{VAR} . The values were determined using formulas given in [69]. The optimized values are $RP1=RP2=RP3=RP4=3997\Omega$, $CP1=CP2=CP3=CP4=0.13\text{ pF}$, $LP1=LP2=LP3=LP4=1.29\text{ nH}$, $CS1=CS2=8.7\text{ pF}$, $LPN=0.21\text{ nH}$, $CVAR=9.6\text{ pF}$, 6.3 pF , 4.6 pF .

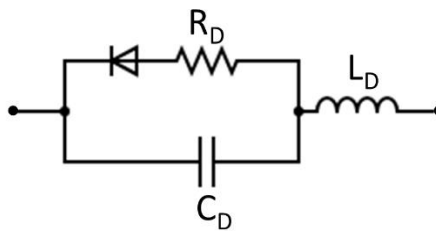


Figure 25: Equivalent model for SMV1234 varactor diode

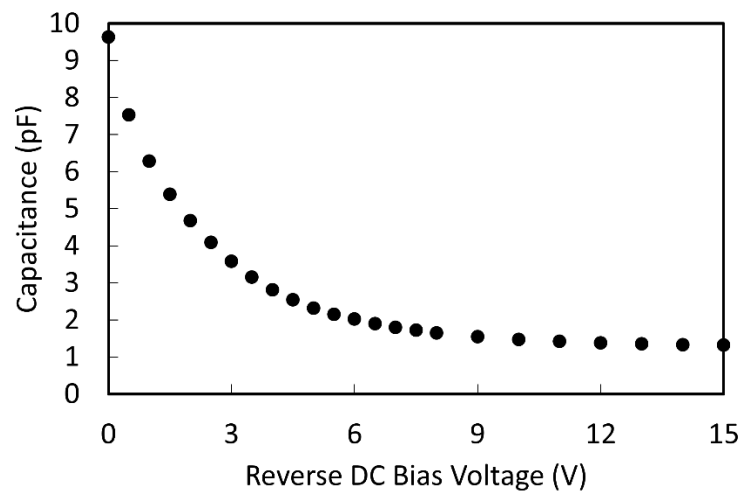


Figure 26: Tuned capacitance versus applied voltage of the SMV1234

A comparison of the resonant frequency versus varactor diode capacitance of the CST simulation and the circuit model is shown in Figure 30, together with the

percentage error for each case. The two models show agreement and consistency with the qualitative explanation discussed during antenna development section. A maximum error of 2.59 % is obtained for 1.7 pF capacitance. The discrepancies can be attributed to the approximate values of the lumped circuit elements. In practice, the lumped element values vary from ideal values and incorporate some additional parasitic capacitance. The divergences are negligibly small and antenna simulation agrees the antenna design theory. The circuit model can be used for quick design using simple circuit analysis techniques.

The simulated axial ratio versus θ for different bias voltages is shown in Figure 31. At boresight, the antenna exhibits linear polarization for 0 V and 1 V bias voltages and elliptical for the others. Between $\theta = 10^\circ$ and $\theta = 40^\circ$, the antenna demonstrates circular polarization for 0 V, 1 V and 2 V, and shows elliptical polarization for 5.5 V and 7.5 V.

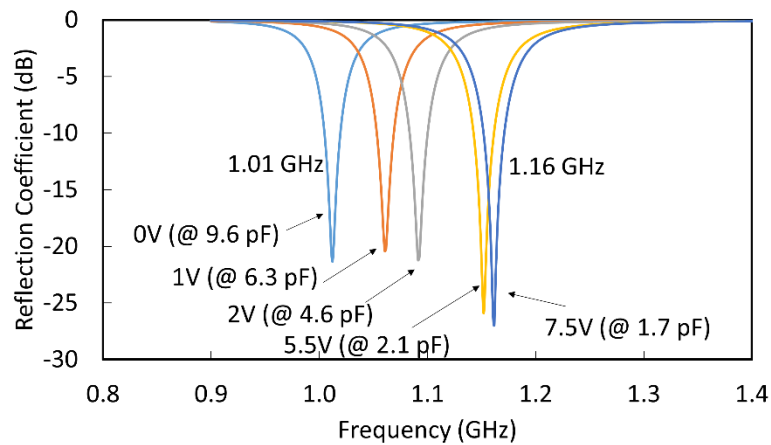


Figure 27: Variation in CST simulated reflection coefficient for different applied DC voltage bias levels

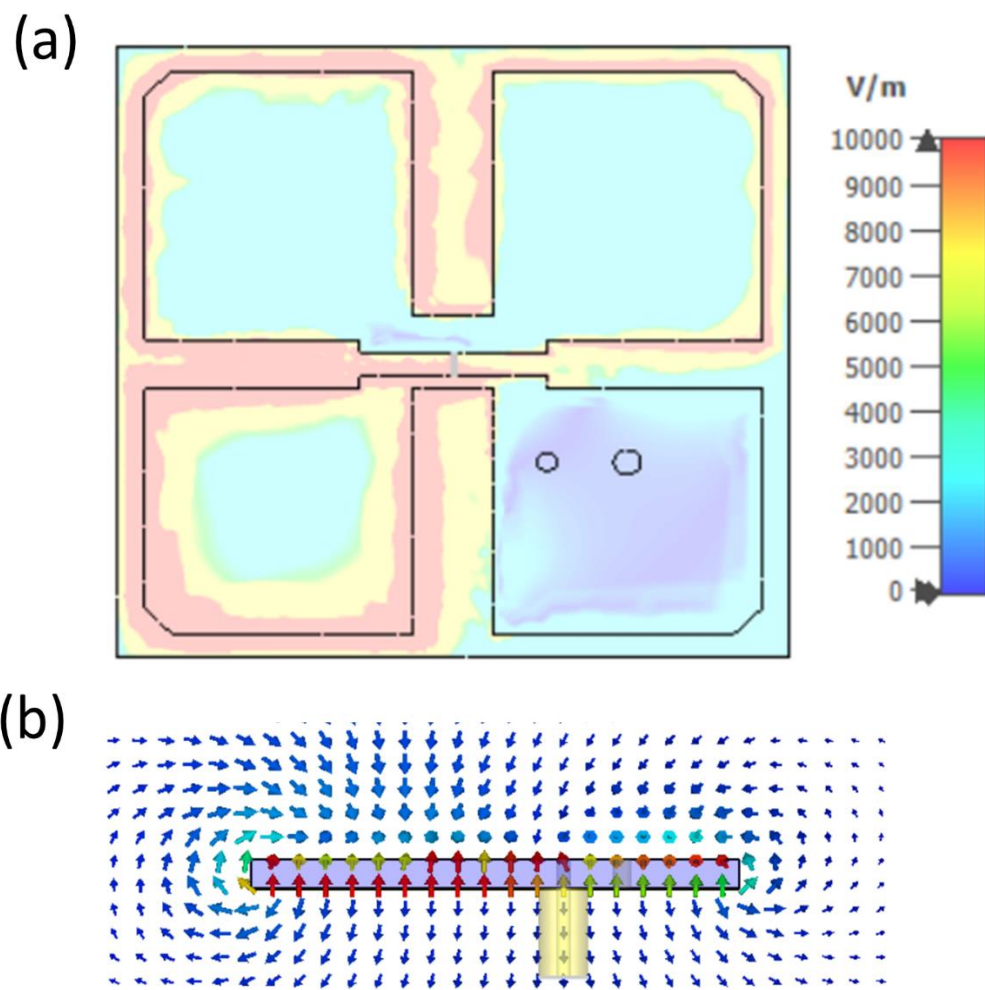


Figure 28: Electromagnetic field distribution at zero bias for (a) xy plane at $z = 1.67$ mm and (b) xz planes at $y=0$ mm

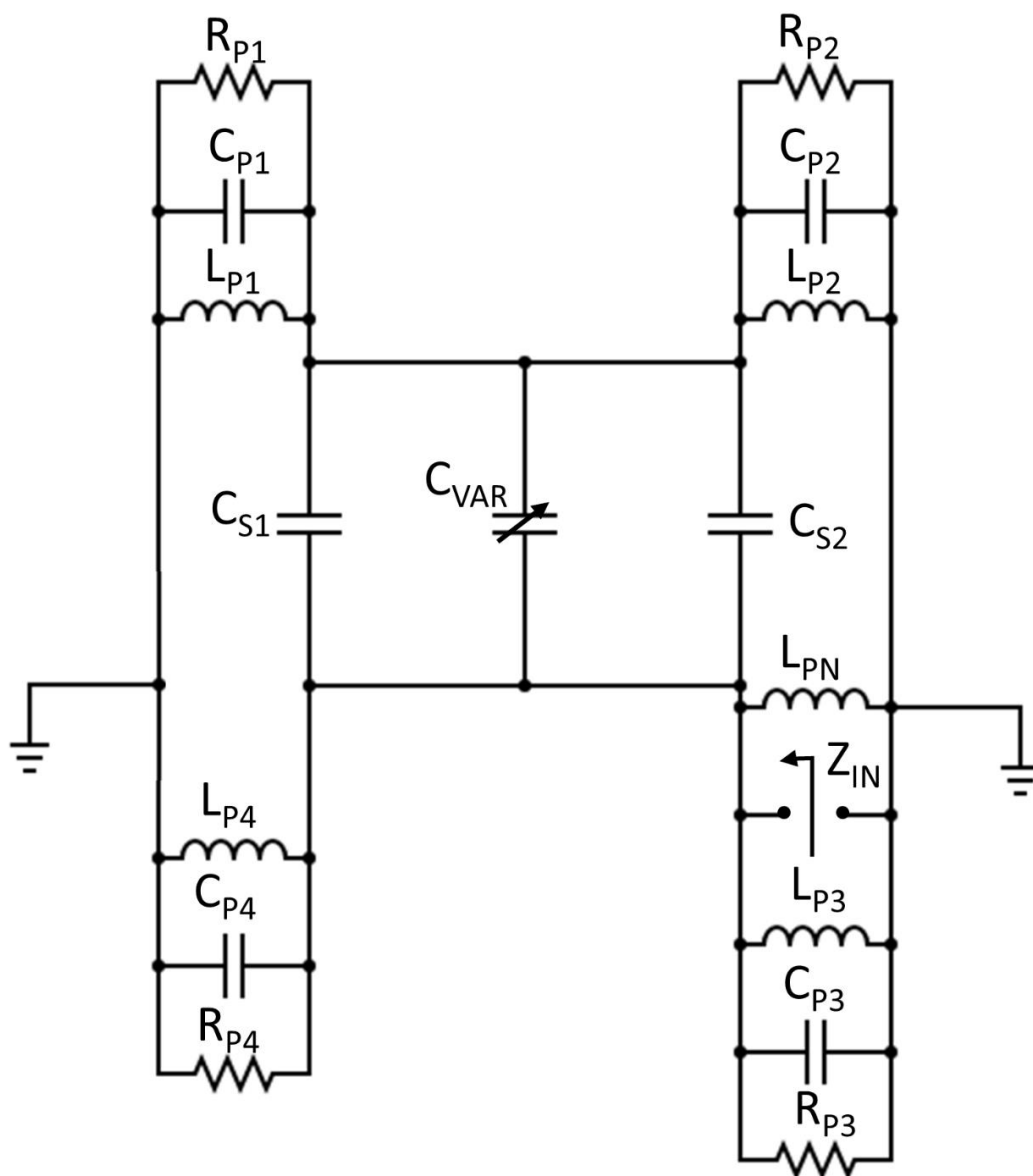


Figure 29: Frequency reconfigurable antenna equivalent circuit

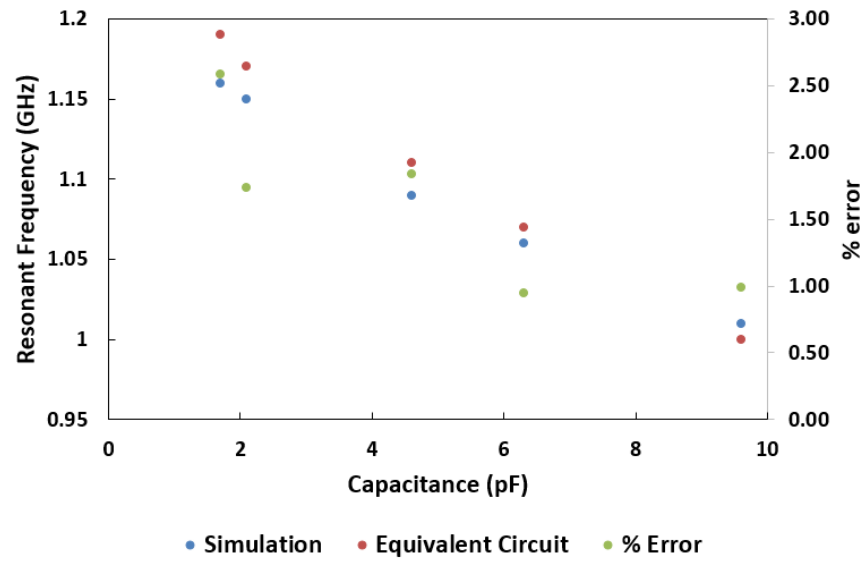


Figure 30: Comparison of resonant frequency from CST simulation and circuit model with corresponding percentage error

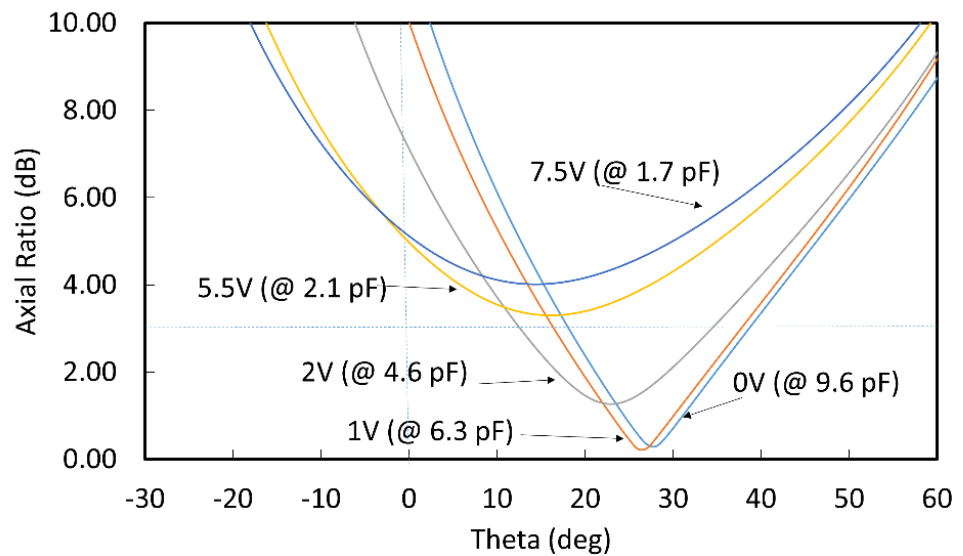


Figure 31: CST simulation results of axial ratio versus θ at $\Phi = 0$ for varying bias voltages

4.3 Antenna Experimental Setup and Measurement

The reflection coefficient values for different biasing voltages were measured using the Rohde and Schwarz R&S®ZVL vector network analyser [70] using a setup as depicted in Figure 32. The RF measurement system was calibrated using the SLOT method [71]. The external biasing DC voltage was applied using DC source connected via a Bias Tee. The Bias Tee applies the RF signal and DC signal simultaneously, to the SMA connector of the antenna as highlighted in Figure 32(b). A Bias Tee is a diplexer with an ideal capacitor that allows AC while blocking DC bias and an ideal inductor that blocks AC while allowing DC. The Bias Tee provides the DC bias voltage required to tune the antenna without mixing with RF signal. The top and bottom of the fabricated antenna are shown in Figure 33 (a) and (b) respectively. The biasing scheme is also shown in Figure 33 (a), with the voltage applied between pad (+) and pad (-). The antenna reflection coefficient and radiation patterns were measured and recorded at 0 V, 1 V, 2 V, 5.5 V and 7.5 V. Anechoic chamber was used for the cut planes and far field measurements as depicted in Figure 34.

4.4 Reflection Coefficient Measurements and Analysis

The measured reflection coefficient versus frequency for the different applied bias voltages depicted in Figure 35 shows a 15% tuning range with the resonant frequency varying from 1.00 GHz to 1.15 GHz as the voltage bias level is increased from 0 V to 7.5 V, agreeing well with the simulated values.

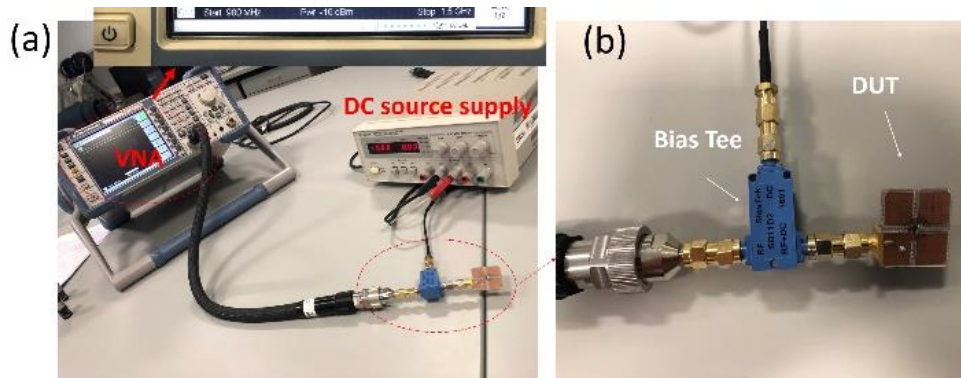


Figure 32: Reflection coefficient measurement (a) measurement setup with the vector network analyzer (b) the Bias Tee connection

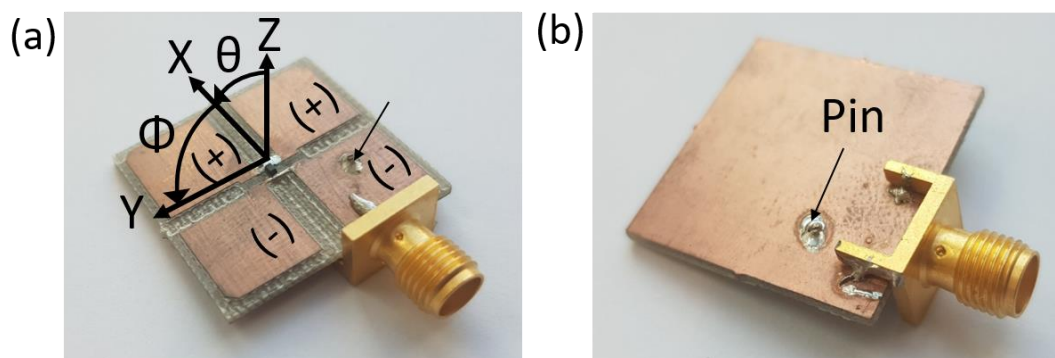


Figure 33: Fabricated antenna (a) perspective view of top (b) perspective view of ground showing inductive pin

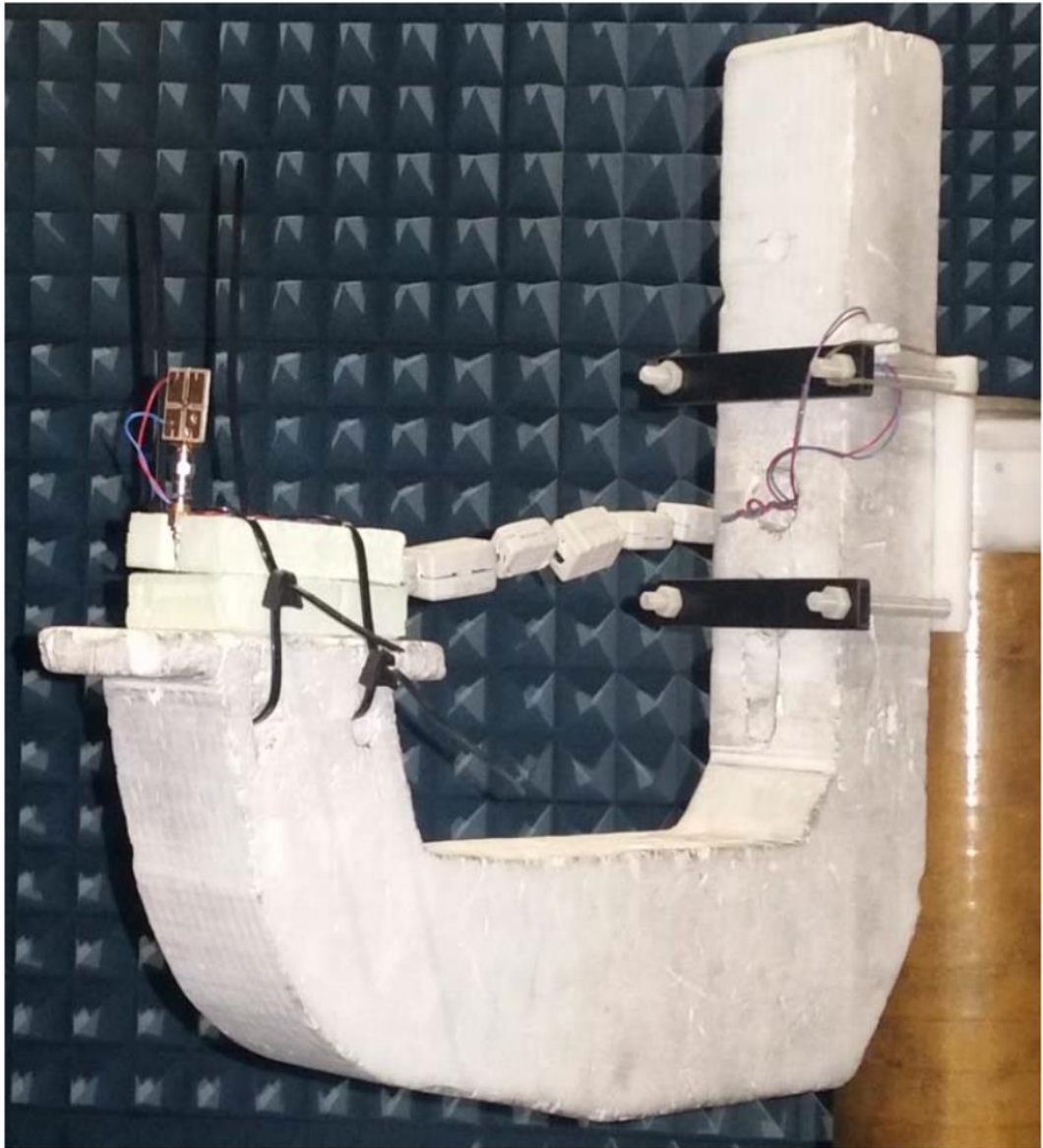


Figure 34: Antenna under test on Roll-over-Azimuth positioner in anechoic chamber at IMST

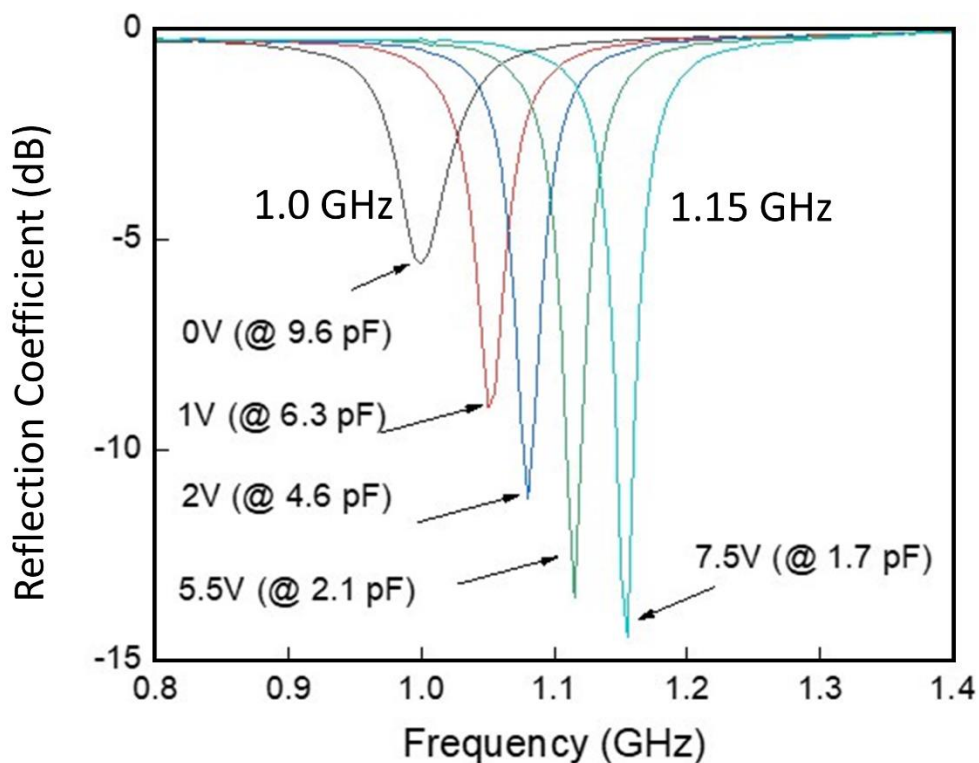


Figure 35: Frequency reconfigurable antenna measured reflection coefficient versus frequency for different applied DC bias voltage levels

Since, in general, the resonant frequency is inversely proportional to the square root of the capacitance [61], the resonance frequency-voltage dependence similarly exhibits a nonlinear relationship. Also, as expected, the matching improves as the resonant frequency increases. The measured return loss is however poorer than the simulated values. This can be attributed to fabrication tolerances and ideality of the diode model used in simulation, which may not accurately capture the effect of all the diode parasitic. Nevertheless, the return loss is less than -6 dB across all the frequency bands. For better matching, an external matching circuit can be employed. The simulated resonant frequency varies from 1.01 GHz to 1.16 GHz with the application of a DC voltage from 0 V to 7.5 V respectively. The measured resonant frequency also follows the same trend. The measured resonant frequency varies between 1 GHz to

1.15 GHz with respect to the DC bias change of 0 V to 15 V respectively. The differences between simulated and measured resonant frequency of the antenna along with the % of error is tabulated in Table 3. There are some variations in resonant frequency of the measured and simulated values. But the tuning ratio is 15 % in both the cases. The inconsistency in part attributed to fabrication tolerances which cause discrepancies in patch and slot sizes. The discrepancies due to fabrication could be improved in future by using chemical etching rather than mechanical milling, which can provide more accurate performance. The variation is also attributed to the practical varactor capacitance values which shift away from the ideal case. This is particularly noticeable for the 5.5 V bias voltage where the varactor capacitance was found to be slightly higher.

Table 3: Comparison between simulated and measured resonant frequency

CAP (pF)	Frequency Simulated (GHz)	Frequency Measured (GHz)	Error (%)
9.6	1.01	1	0.99
6.3	1.06	1.05	0.94
4.6	1.09	1.08	0.92
2.1	1.15	1.12	2.61
1.7	1.16	1.15	0.86

4.5 Far-Field Measurements and Analysis

The far-field measurements were carried out in air-conditioned and a completely shielded anechoic chamber (Range I). This is to minimize the measurements error caused by variation in temperature, interference signals and reflections. The antenna was setup at a far field distance of approximately of 7.5 meters. The accuracy of the azimuth positioner is 0.03° . To minimize errors caused by

mismatch, the feeding cable was equipped with an attenuator with very low VSWR. The accuracy of the far field measurements was set to ± 1 dB.

The normalised simulated and measured co-polarisation cross polarisation radiation patterns of the reconfigurable antenna at 1000 MHz, which corresponds to zero bias are, shown Figure 36. The co-polarization and cross-polarization radiation patterns are plotted for the xz and yz propagation planes. The simulated co and cross polarization gives very good results as shown in Figure 36 (a) and (c), which is particularly evident for yz plane. The far field antenna measurement has some discrepancy with the simulation results. The antenna has high measured cross polarization. Rectangular patch antenna radiates mainly in linearly polarized fields along broadside direction. There is a chance of cross polarization which prominent in H plane than in E plane [72]. This is due to the higher order orthogonal modes in the antenna. Different innovative feeding techniques are reported in literature which can improve the cross polarization [73, 74]. The antenna has the best polarization purity at $\theta = 0^\circ$ in the xz plane. The shape of the radiation patterns can also be attributed to the small ground plane size which extends only 2 mm and 1.5 mm beyond the patch in the x and y directions respectively. A larger ground plane results in a unidirectional radiation pattern, 40° reduction in half power beam width and 5 dB increase in gain. Different innovative feeding techniques are reported in literature which can improve the cross polarization.

The normalized simulated and measured absolute gain radiation patterns are shown in Figure 37 for the xz plane ((a), (b)) and yz plane ((c), (d)), for different applied bias voltages. With increase in voltage from 0 V to 7.5 V, the field distribution increases along the main lobe direction and the antenna is tuned. As the frequency goes

higher, keeping same physical dimensions, the mutual coupling decreases, which attributed to the cut pattern shape. The simulated and measured radiation pattern differs in pattern shape. This difference is due to the addition of large bias cable inserted in the antenna between the bias points as shown in Figure 34. For far field measurement Bias Tee is not used, so noise from the DC power supply does appear on the signal line, which results in the dissimilarity between measured and simulated results. This can be improved by proper biasing techniques like incorporation of the Bias Tee, of isolation of DC bias and RF signal.

The realized gain of the antenna is less than 0 dBi. This can be improved by increasing substrate thickness, using a low loss substrate and using a biasing scheme that allows for isolation of the DC bias and RF signals or mounting the antenna over a large ground plane. Axial ratio measurement done at boresight showed that the antenna exhibits linear polarization for all bias voltages.

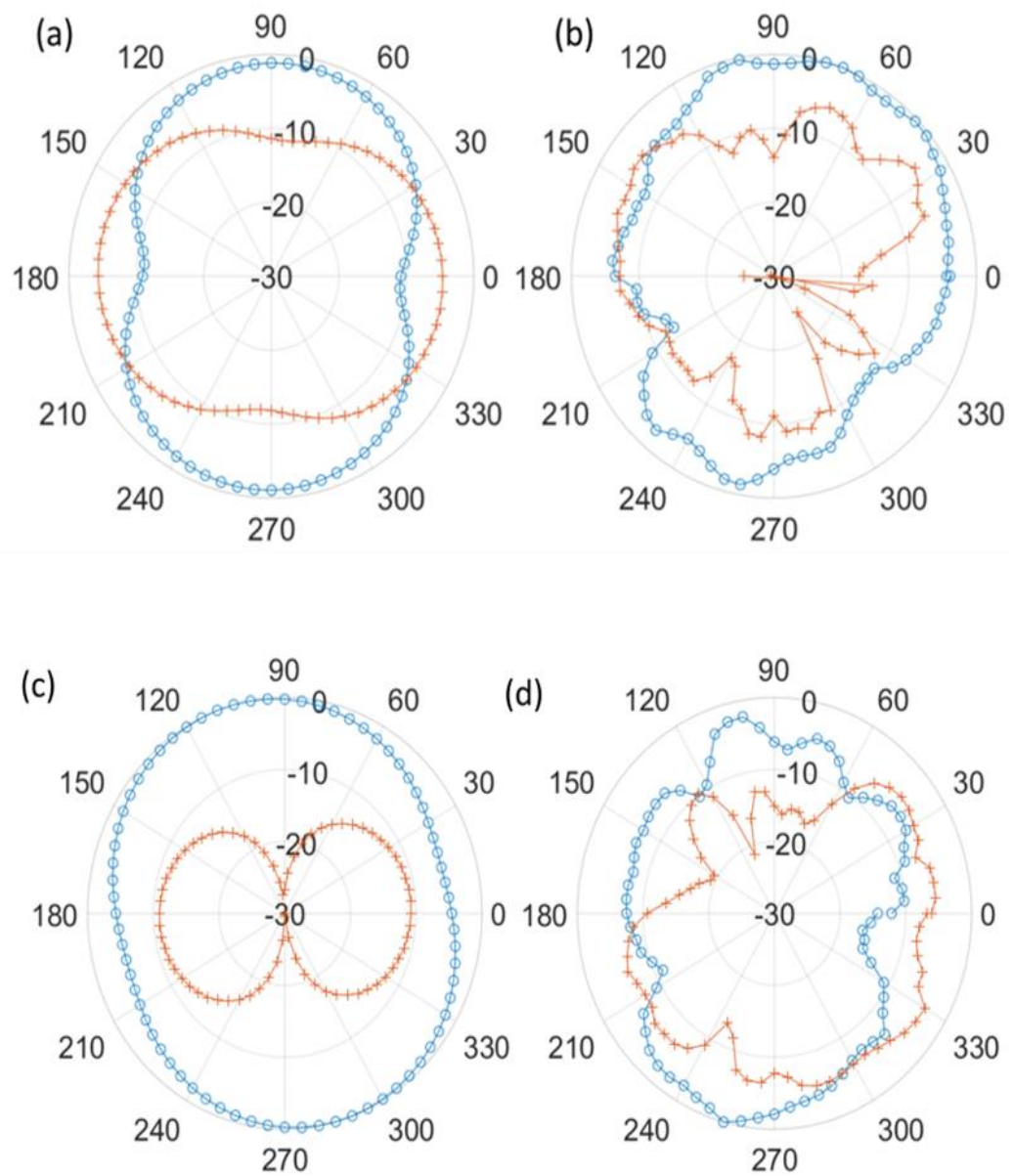


Figure 36: Normalized gain radiation pattern of the antenna at zero bias (a) simulated (CST) in xz plane, (b) measured in xz plane, (c) simulated (CST) in yz plane and (d) measured in yz plane at 1000 MHz. (o corresponds for co-polarization, + corresponds for cross-polarization)

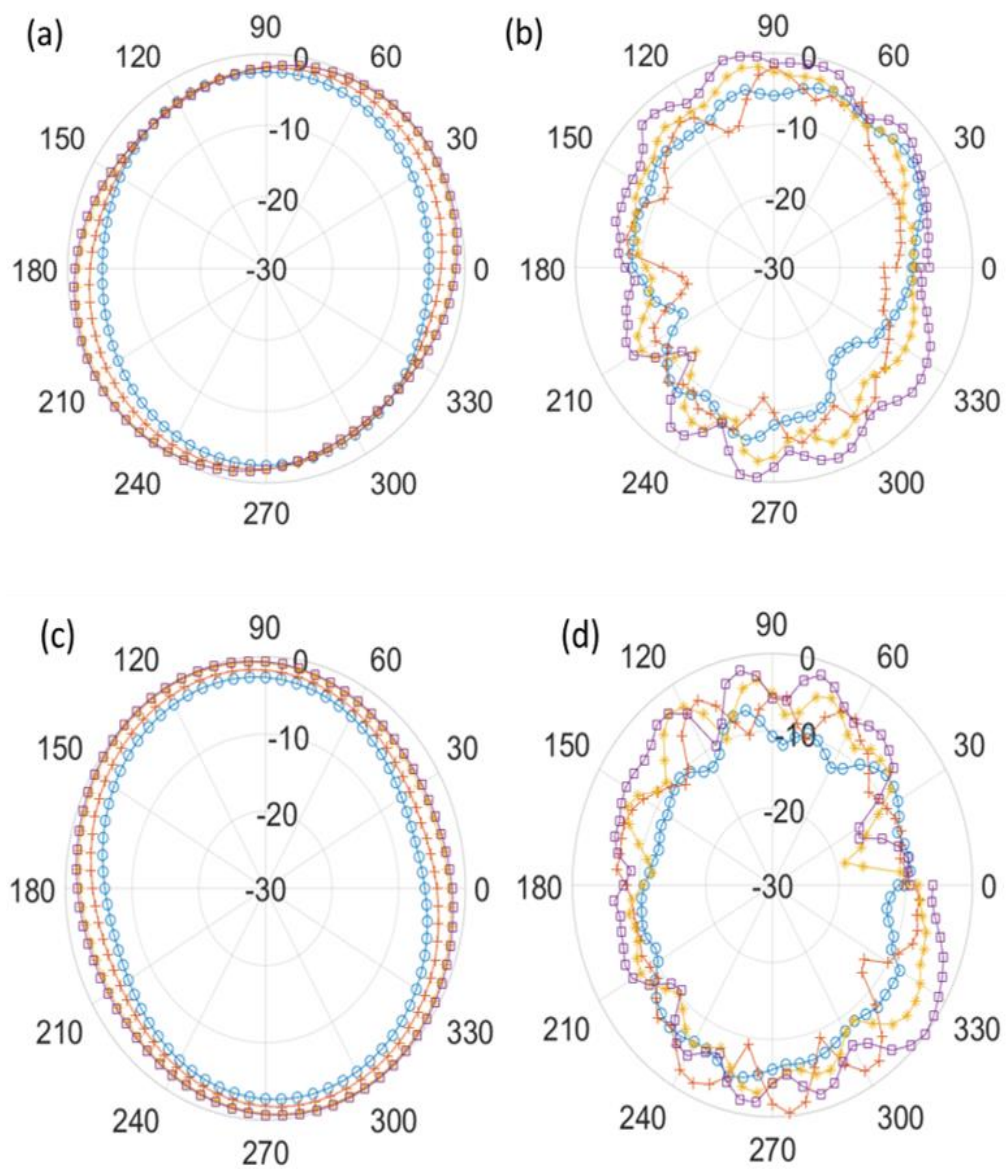


Figure 37: Normalized absolute gain radiation patterns plots (a) simulated (CST) xz plane (b) measured xz plane and (c) simulated (CST) yz plane and (d) measured yz plane for different applied bias voltages. (o corresponds to zero bias (1000 MHz), + corresponds to 2 V bias (1080 MHz), *corresponds to 5.5 V bias (1130 MHz), □ corresponds to 7.5 V bias (1150 MHz))

A comparison of the proposed antenna with state-of-the-art frequency reconfigurable antennas employing varactor diodes is highlighted in Table 4. The design uses a single varactor which is the minimum number of varactors employed in all the literature. The antenna compactness is particularly evident considering that the

antenna frequency range is towards the lower end of the spectrum highlighted. In particular, the antennas in references [75-77] were also designed for compactness and operate in the same or nearby frequency ranges. The proposed antenna has a distinctly smaller overall size.

Table 4: Comparison of proposed design with reported works employing varactor diodes

Ref	No. of diode	Varactor model	Frequency range (MHz)	Tuning ratio	Bias voltage (V)	Capacitance variation (pF)	Structure size (mm)
[33]	1	SMV 2019	690 to 804, 1704 to 2268	1.16 1.32	0 to 20	2.25 to 0.16	44 x 134 x 8
[39]	1	JZ060	2200 to 2600	1.18	NA	6 to 2	41.8 x 49.4 x 0.79
[40]	4	SMV 2020	1470 to 1840	1.25	0 to 20	7 to 0.4	> 87 x 148 x 3.2
[42]	2	BB85	3280 to 3510 5470 to 6030	1.07 1.1	0 to 30	7 to 0.4	40 x 40 x 0.764
[75]	2	GC 15006	410 to 990	2.41	0 to 20	1.8 to 0.14	460 x 410 x 4.77
		GC 15011	2100 to 3500	1.67	0 to 20	50 to 4.1	
[76]	1	SMTD 3001	1370 to 1680	1.23	0 to 30	2.2 to 0.5	26 x 26 x 1.5
[77]	1	BB184	550 to 1500	2.73	1 to 10	14 to 2	80 x 40 x 1.524
This work	1	SMV 1234	1000 to 1150	1.15	0 to 7.5	9.63 to 1.72	22 x 21 x 1.6

The use of a single varactor diode and small size have lower cost implications, especially in the case of large-scale manufacture. The tuning ratio of the proposed antenna is comparable to that of reported works. Most of the reported work achieves frequency tunability at the middle of the L band spectrum and not covering the lower end of the spectrum. The proposed antenna also has a lower bias voltage requirement of 7.5 V which is less than all the reported work. Majority of the reported work uses a

DC bias of above 20 V to achieve the frequency tunability. Antenna reported in reference [77] has lower bias requirement and good tuning ratio, but the size of the antenna is very high compared to proposed antenna.

In summary, the proposed design is compact and achieves frequency reconfiguration, with a single varactor diode and a low bias voltage requirement as compared to reported works.

Chapter 5: Outlook and Conclusions

5.1 Conclusions

To address the need for smart solutions that can efficiently utilize a shared communication medium, taking into account the increasing demand for wireless communication services and applications, a system architecture for wireless multiplexing using a tunable antenna has been proposed. Although user requirements are generally fixed, dynamic spectrum allocation is necessary to optimally use the communication media. The proposed architecture enables this through frequency reconfiguration. Two units of this architecture were designed, implemented in hardware, and tested; a wireless multiplexing agile antenna-based control system and a frequency reconfigurable antenna. They were designed for space application and operation in the 1 to 2 GHz frequency band.

The wireless multiplexing agile antenna-based control acts as a biasing and control circuit/system. The hardware implementation of this device comprises a microcontroller, DAC, CMOS oscillator, power module, and a USB interface for communication with custom-built software installed on a PC. It has functions for control, digital signal processing, and de-multiplexing. To demonstrate its performance, an input multiplexed signal was de-multiplexed into its constituent signals and displayed on the software interface. The device is programmable and a variety of voltage bias levels can be configured, therefore the device can provide a cost-effective and flexible solution for a variety of real-world applications.

The frequency reconfigurable antenna is a compact design that employs a single varactor diode. The varactor capacitance was varied from 9.6 pF to 1.7 pF with the application of maximum DC reverse bias of 7.5 V. The resonant frequency of the antenna fabricated on an FR4 substrate was correspondingly tuned from 1000 MHz to 1150 MHz, resulting in a 15% tuning range. With increased DC bias voltage, the field distribution increases along the main lobe direction. The proposed antenna design demonstrates, tuning feasibility, comparable tuning ratio, and device significant compactness as compared to reported works. The demonstrated frequency tunable antenna can provide enhanced functionality by providing the wireless terminals or handset with more frequency bands and bandwidth, maintaining the compact size, and reducing the interference and can find application in various existing and emerging communication systems.

A future extension of this work is to design the other elements of the RF front end, incorporate all elements of the system architecture, and carry out end-to-end performance testing. The tests will include a detailed analysis of power consumption, the effect of frequency/bias switching on system performance, and a comparison of performance with separate circuitry for different frequencies.

To the best of this author's knowledge, at the time of this writing, and there is no commercially available multiplexing solution or proposed literature that utilizes a frequency tunable/agile antenna.

5.2 Outlook

For proof of concept and due cost implications, the hardware modules that were implemented were designed on FR4 board using standard PCB design, fabrication, and

assembly techniques. However, as the development of this architecture is targeted for space application, future iterations will require the use of high-quality qualified materials that can ensure high-reliability performance. The materials should have very good electrical properties and be able to operate in the harsh environment of space. Additionally, radiation-hardened packaging will have to be employed to provide shielding protection to avoid damage or malfunctioning due to ionizing radiation.

The system must continue to operate under extreme conditions during satellite launch and flight in space. During the launch, the PCB material and packing should be able to handle the shock and stresses and to provide some damping to avoid lead disconnects due to the heavy vibration. It should be able to withstand high radiation and sudden changes in temperature that are characteristic of space.

It is also important that the device be able to operate for extended periods. This can be done by optimizing component selection and adherence to the relevant space standards. Selecting components from certified contract manufacturers, with the required thermal ratings and that can withstand the environmental conditions can significantly extend the device lifetime. Specialized testing of the device's electrical, mechanical and thermal performance would be needed to verify device operation in space.

A modular approach was adopted for the development of the system architecture for wireless multiplexing using a tunable antenna. This was to enable independent testing and verification of the different units. From the commercialization aspect, this can introduce the element of flexibility as various modules can be interchanged to meet requirements provided modular standards are established. The proposed system architecture can provide a commercially viable solution for

frequency-agile wireless multiplexing in space, provided the more stringent PCB requirements for space applications discussed above are taken into consideration.

An electronically tunable transmitting and receiving antennas are considered to be an excellent solution for multiband software-defined radio (SDR) implementations. SDR finds potential applications in military and wireless communications including hand-held, airborne, vehicular, and dismounted radios. Nevertheless, due to the requirement of a complex wideband or multiband antenna, the use of SDRs over large frequency bands is limited at the RF front-end. The RF front-end can be optimized by properly using an inherently narrowband tunable antenna whose frequency characteristics can be continuously regulated by some tuning action like electronic tuning, making it much easier to achieve the frequency agility needed for multi-band SDRs. The tunable antenna can be controlled by a microcontroller as discussed in the WAM controller design. Incorporation of tunable antennas in transmitter and receiver, in turn, abridging the overall analog filters in the RF front-end and thus the overall design issue.

References

- [1] Y. Songnan, Z. Chunna, H. K. Pan, A. E. Fathy, and V. K. Nair, "Frequency-Reconfigurable Antennas for Multiradio Wireless Platforms," *IEEE Microwave Magazine*, vol. 10, no. 1, pp. 66-83, 2009.
- [2] N. Nguyen-Trong, L. Hall, and C. Fumeaux, "A Frequency- and Pattern-Reconfigurable Center-Shorted Microstrip Antenna," *IEEE Antennas and Wireless Propagation Letters*, vol. 15, pp. 1955-1958, 2016.
- [3] C. Mao, S. Gao, Y. Wang, and B. Sanz-Izquierdo, "A Novel Multiband Directional Antenna for Wireless Communications," *IEEE Antennas and Wireless Propagation Letters*, vol. 16, pp. 1217-1220, 2017.
- [4] A. Boukarkar, X. Q. Lin, Y. Jiang, and Y. Q. Yu, "Miniaturized Single-Feed Multiband Patch Antennas," *IEEE Transactions on Antennas and Propagation*, vol. 65, no. 2, pp. 850-854, 2017.
- [5] A. W. M. Saadh and R. Poonkuzhali, "A compact CPW fed multiband antenna for WLAN/INSAT/WPAN applications," *AEU - International Journal of Electronics and Communications*, vol. 109, pp. 128-135, 2019.
- [6] K. M. Mak, H. W. Lai, and K. M. Luk, "A 5G Wideband Patch Antenna With Antisymmetric L-shaped Probe Feeds," *IEEE Transactions on Antennas and Propagation*, vol. 66, no. 2, pp. 957-961, 2018.
- [7] Q. Liu, L. Zhu, J. Wang, and W. Wu, "A Wideband Patch and SIW Cavity Hybrid Antenna With Filtering Response," *IEEE Antennas and Wireless Propagation Letters*, vol. 19, no. 5, pp. 836-840, 2020.
- [8] B. Chen, X. Yang, and D. Hu, "Fish-shaped ultra-wideband patch antenna with tilt-folded patch feed," *IET Microwaves, Antennas & Propagation*, vol. 13, no. 9, pp. 1312-1317, 2019.
- [9] S. N. M. Zainarry, N. Nguyen-Trong, and C. Fumeaux, "A Frequency- and Pattern-Reconfigurable Two-Element Array Antenna," *IEEE Antennas and Wireless Propagation Letters*, vol. 17, no. 4, pp. 617-620, 2018.
- [10] Y. Cai, K. Li, Y. Yin, S. Gao, W. Hu, and L. Zhao, "A Low-Profile Frequency Reconfigurable Grid-Slotted Patch Antenna," *IEEE Access*, vol. 6, pp. 36305-36312, 2018.
- [11] K. Aslanidis and V. N. Gunasegaran "TRF7970A NFC Reader Antenna Multiplexing," T. Instruments, Ed., ed. Texas, 2016.

- [12] "Airmux-400 Broadband Wireless Multiplexer (Ver. 2.4)," T. A. Company, Ed., 2.4 ed.
- [13] A. J. Paulraj and T. Kailath, "Increasing capacity in wireless broadcast systems using distributed transmission/directional reception (DTDR)," 1994.
- [14] R. W. Chang, "Synthesis of band-limited orthogonal signals for multichannel data transmission," *The Bell System Technical Journal*, vol. 45, no. 10, pp. 1775-1796, 1966.
- [15] S. Weinstein and P. Ebert, "Data Transmission by Frequency-Division Multiplexing Using the Discrete Fourier Transform," *IEEE Transactions on Communication Technology*, vol. 19, no. 5, pp. 628-634, 1971.
- [16] H. Sari, Y. Levy, and G. Karam, "An analysis of orthogonal frequency-division multiple access," in *GLOBECOM 97. IEEE Global Telecommunications Conference. Conference Record*, vol. 3, pp. 1635-1639, 1997
- [17] C. Wang and K. Chang, "Microstrip multiplexer with four channels for broadband system applications," *International Journal of RF and Microwave Computer-Aided Engineering*, vol. 11, no. 1, pp. 48-54, 2001.
- [18] M. Rais-Zadeh, J. T. Fox, D. D. Wentzloff, and Y. B. Gianchandani, "Reconfigurable Radios: A Possible Solution to Reduce Entry Costs in Wireless Phones," *Proceedings of the IEEE*, vol. 103, no. 3, pp. 438-451, 2015.
- [19] P. Bhartia and I. Bahl, "A frequency agile microstrip antenna," *Antennas and Propagation Society International Symposium*, vol. 20, pp. 304-307, 1982.
- [20] I. T. Elfergani, J. Rodriguez, I. Otung, W. Mshwat, and R. A. Abd-Alhameed, "Slotted Printed Monopole UWB Antennas with Tuneable Rejection Bands for WLAN/WiMAX and X-Band Coexistence," *Radioengineering*, vol. 27, no. 3, pp. 694-702, 2018.
- [21] Y. Yashchyshyn, "Reconfigurable antennas: the state of the art," *Int. J. Electron. Telecommun.*, vol. 56, pp. 319-326, 2010
- [22] A. Petosa, "An Overview of Tuning Techniques for Frequency-Agile Antennas," *IEEE Antennas and Propagation Magazine*, vol. 54, no. 5, pp. 271-296, 2012.
- [23] C. G. Christodoulou, Y. Tawk, S. A. Lane, and S. R. Erwin, "Reconfigurable Antennas for Wireless and Space Applications," *Proceedings of the IEEE*, vol. 100, no. 7, pp. 2250-2261, 2012.

- [24] V. Nasserddine, "Millimeter-wave phase shifters based on tunable transmission lines in MEMS technology post-CMOS process." *Université Grenoble Alpes*, 2016.
- [25] H. Campanella, "Tunable FBARs: Frequency tuning mechanisms," in *The 40th European Microwave Conference*, pp. 795-798, 2010.
- [26] F. C. W. Po, E. de Foucauld, J.-B. David, C. Delavaud, and P. Ciaï, "An Efficient Adaptive Antenna-Impedance Tuning Unit Designed for Wireless Pacemaker Telemetry" *InTech, Modern Telemetry*, 2011.
- [27] L. Huang and P. Russer, "Electrically Tunable Antenna Design Procedure for Mobile Applications," *IEEE Transactions on Microwave Theory and Techniques*, vol. 56, no. 12, pp. 2789-2797, 2008.
- [28] G. Upadhyay, N. Kishore, P. Ranjan, V. Tripathi, and S. Tripathi, "Frequency Reconfigurable Multiband Patch Antenna Using PIN-Diode for ITS Applications," *International Journal of Electronics and Communication Engineering*, vol. 12, no. 10, pp. 735-739, 2018.
- [29] T. Li, H. Zhai, X. Wang, L. Li, and C. Liang, "Frequency-Reconfigurable Bow-Tie Antenna for Bluetooth, WiMAX, and WLAN Applications," *IEEE Antennas and Wireless Propagation Letters*, vol. 14, pp. 171-174, 2015.
- [30] N. Symeon, R. Bairavasubramanian, C. Lugo, I. Carrasquillo, D. C. Thompson, G.E. Ponchak, J. Papapolymerou and M.M. Tentzeris , "Pattern and frequency reconfigurable annular slot antenna using PIN diodes," *IEEE Transactions on Antennas and Propagation*, vol. 54, no. 2, pp. 439-448, 2006.
- [31] D. E. Anagnostou and A. A. Gheethan, "A Coplanar Reconfigurable Folded Slot Antenna Without Bias Network for WLAN Applications," *IEEE Antennas and Wireless Propagation Letters*, vol. 8, pp. 1057-1060, 2009.
- [32] H. T. Chattha, N. Aftab, M. Akram, N. Sheriff, Y. Huang, and Q. H. Abbasi, "Frequency reconfigurable patch antenna with bias tee for wireless LAN applications," *IET Microwaves, Antennas & Propagation*, vol. 12, no. 14, pp. 2248-2254, 2018.
- [33] C. Yoon, S.-G. Hwang, G.-C. Lee, W.-S. kim, H.-C. Lee, and H.-D. Park, "A reconfigurable antenna using varactor diode for LTE MIMO applications," *Microwave and Optical Technology Letters*, vol. 55, no. 5, pp. 1141-1145, 2013.
- [34] S. V. Hum and H. Y. Xiong, "Analysis and Design of a Differentially-Fed Frequency Agile Microstrip Patch Antenna," *IEEE Transactions on Antennas and Propagation*, vol. 58, no. 10, pp. 3122-3130, 2010.

- [35] L. Huitema, T. Reveyrand, J. Mattei, E. Arnaud, C. Decroze, and T. Monediere, "Frequency Tunable Antenna Using a Magneto-Dielectric Material for DVB-H Application," *IEEE Transactions on Antennas and Propagation*, vol. 61, no. 9, pp. 4456-4466, 2013.
- [36] P. Pujari and K. Vyas, and B.K. Sharma "Reconfigurable Antenna (Circular Micro strip Patch Antenna) Using Varactor Diodes," *International Journal of Advanced Research in Computer Science*, vol. 4, no. 3, 2017.
- [37] J. Zhang and A. Mortazawi, "An L-band tunable microstrip antenna using multiple varactors," in *IEEE Antennas and Propagation Society International Symposium. Digest. Held in conjunction with: USNC/CNC/URSI North American Radio Sci. Meeting (Cat. No.03CH37450)*, vol. 4, pp. 524-527, 2003.
- [38] A. P. Deo, A. Sonker, and R. Kumar, "Design of reconfigurable slot antenna using varactor diode," in *2017 International Conference on Computer, Communications and Electronics (Comptelix)*, pp. 511-515, 2017.
- [39] R. Khelladi, F. Ghanem, M. Djeddou, and S. Tedjini, "Design of Narrowband Frequency-Tunable Antenna," in *2018 2nd URSI Atlantic Radio Science Meeting (AT-RASC)*, pp. 1-3, 2018.
- [40] F. Meng, S. K. Sharma, and B. Babakhani, "A wideband frequency agile fork-shaped microstrip patch antenna with nearly invariant radiation patterns," *International Journal of RF and Microwave Computer-Aided Engineering*, vol. 26, no. 7, pp. 623-632, 2016.
- [41] M. N. M. Kehn, Ó. Quevedo-Teruel, and E. Rajo-Iglesias, "Reconfigurable loaded planar inverted-F antenna using varactor diodes," *IEEE Antennas and Wireless Propagation Letters*, vol. 10, pp. 466-468, 2011.
- [42] A. Boukarkar, X. Q. Lin, and Y. Jiang, "A Dual-Band Frequency-Tunable Magnetic Dipole Antenna for WiMAX/WLAN Applications," *IEEE Antennas and Wireless Propagation Letters*, vol. 15, pp. 492-495, 2016.
- [43] N. Behdad and K. Sarabandi, "A varactor-tuned dual-band slot antenna," *IEEE Transactions on Antennas and Propagation*, vol. 54, no. 2, pp. 401-408, 2006.
- [44] A. Khidre, F. Yang, and A. Z. Elsherbeni, "A Patch Antenna With a Varactor-Loaded Slot for Reconfigurable Dual-Band Operation," *IEEE Transactions on Antennas and Propagation*, vol. 63, no. 2, pp. 755-760, 2015.
- [45] B. R. Holland, R. Ramadoss, S. Pandey, and P. Agrawal, "Tunable coplanar patch antenna using varactor," *Electronics Letters*, vol. 42, no. 6, pp. 319-321. Available: https://digital-library.theiet.org/content/journals/10.1049/el_20063554

- [46] J. A. Garcia, L. Cabria, and A. Mediavilla, "A Frequency Agile Phase-Conjugating Active Antenna for Full-Duplex Retrodirective Arrays," in *2006 IEEE MTT-S International Microwave Symposium Digest*, 2006, pp. 622-625.
- [47] Y. Turki and R. Staraj, "CPW-fed frequency-agile shorted patch," *Microwave and Optical Technology Letters*, vol. 25, no. 5, pp. 291-294, 2000.
- [48] M. A. Madi, M. Al-Husseini, and M. Y. Mervat, "Frequency Tunable Cedar-Shaped Antenna for WiFi and WiMAX," *Progress In Electromagnetics Research Letters*, vol. 72, pp. 135-143, 2018.
- [49] A. Sondaş, M. H. B. Uçar, and Y. E. Erdemli, "Tunable loop-loaded printed dipole antenna design," in *2010 IEEE Antennas and Propagation Society International Symposium*, pp. 1-4, 2010.
- [50] Q. Bai, R. Singh, K. L. Ford, T. O'Farrell, and R. J. Langley, "An Independently Tunable Tri-Band Antenna Design for Concurrent Multiband Single Chain Radio Receivers," *IEEE Transactions on Antennas and Propagation*, vol. 65, no. 12, pp. 6290-6297, 2017.
- [51] M. Nejatijahromi, M. Rahman, and M. Naghshvarianjahromi, "Continuously Tunable WiMAX Band-Notched UWB Antenna with Fixed WLAN Notched Band," *Progress In Electromagnetics Research Letters*, vol. 75, pp. 97-103, 2018.
- [52] M. Nejatijahromi, M. Naghshvarianjahromi, and M. Rahman, "Switchable Planar Monopole Antenna Between Ultra-Wideband and Narrow Band Behavior," *Progress In Electromagnetics Research Letters*, vol. 75, pp. 131-137, 2018.
- [53] P. M. Haskins, P. S. Hall, and J. S. Dahele, "Active patch antenna element with diode tuning," *Electronics Letters*, vol. 27, no. 20, pp. 1846-1848, 1991.
- [54] S. Kawasaki and T. Itoh, "A slot antenna with electronically tunable length," *Proc. IEEE International Symposium on Antennas and Propagation*, vol. 1, London, Canada, pp. 130-33, 1991.
- [55] M. D. Wright, W. Baron, J. Miller, J. Tuss, D. Zeppettella, and M. Ali, "MEMS Reconfigurable Broadband Patch Antenna for Conformal Applications," *IEEE Transactions on Antennas and Propagation*, vol. 66, no. 6, pp. 2770-2778, 2018.
- [56] R. Saha, S. Maity, and C. T. Bhunia, "Design and characterization of a tunable patch antenna loaded with capacitive MEMS switch using CSRRs structure on the patch," *Alexandria Engineering Journal*, vol. 55, no. 3, pp. 2621-2630, 2016/09/01/ 2016.

- [57] E. Erdil, K. Topalli, M. Unlu, O. A. Civi, and T. Akin, "Frequency Tunable Microstrip Patch Antenna Using RF MEMS Technology," *IEEE Transactions on Antennas and Propagation*, vol. 55, no. 4, pp. 1193-1196, 2007.
- [58] S. Caporal Del Barrio, A. Morris, and G. F. Pedersen, "Antenna Miniaturization with MEMS Tunable Capacitors: Techniques and Trade-Offs," *International Journal of Antennas and Propagation*, vol. 2014, pp. 1-8, 2014.
- [59] R. Jackson and R. Ramadoss, "A MEMS-based electrostatically tunable circular microstrip patch antenna," *Journal of Micromechanics and Microengineering*, vol. 17, no. 1, pp. 1-8, 2006/11/24 2006.
- [60] H. Nawaz and I. Tekin, "Three dual polarized 2.4GHz microstrip patch antennas for active antenna and in-band full duplex applications," in *2016 16th Mediterranean Microwave Symposium (MMS)*, pp. 1-4, 2016.
- [61] Sedra AS, Sedra DE, Smith KC. "Microelectronic circuits". New York: Oxford University Press, 1998.
- [62] M. Al Ahmad, S. Kabeer, and L. J. Olule, "Wireless Multiplexing Agile Antenna-Based Control System," *IEEE Access*, vol. 9, pp. 9664-9669, 2021.
- [63] Microchip Technology Inc, "PIC32MK1024GPD064." <https://www.microchip.com/wwwproducts/en/PIC32MK1024GPD064>, accessed August 2020.
- [64] Texas Instruments, "DAC7718." <https://www.ti.com/product/DAC7718>, accessed August 2020.
- [65] Kyocera, "KC2520B C1." https://global.kyocera.com/prdct/electro/product/pdf/kc2520b_c1_e.pdf, accessed August 2020.
- [66] J. S. Roy, N. Chattoraj, and N. Swain, "Short-circuited microstrip antennas for multiband wireless communications," *Microwave and Optical Technology Letters*, vol. 48, no. 12, pp. 2372-2375, 2006.
- [67] M. Al Ahmad, S. Kabeer, A. A. Sanad, and L. J. Olule, "Compact single-varactor diode frequency-reconfigurable microstrip patch antenna," *IET Microwaves, Antennas & Propagation*, 2021.
- [68] K. Carver and J. Mink, "Microstrip antenna technology," *IEEE Transactions on Antennas and Propagation*, vol. 29, no. 1, pp. 2-24, 1981.
- [69] R. Garg, I. Bahl, and M. Bozzi, *Microstrip lines and slotlines*. Artech house, 2013.

- [70] Rohde & Schwarz: 'R&S®ZVL vector network analyzer', https://www.rohde-schwarz.com/pt/product/zvl-productstartpage_63493-9014.html, accessed August 2020.
- [71] M. Golio and J. Golio, "RF and microwave circuits, measurements, and modeling", Boca Raton: CRC press, 2018.
- [72] T. Huynh, K. Lee, and R. Lee, "Crosspolarisation characteristics of rectangular patch antennas," *Electronics Letters*, vol. 24, no. 8, pp. 463-464, 1988.
- [73] L. Jong-Sik, K. Chul-Soo, L. Young-Taek, A. Dal, and N. Sangwook, "A spiral-shaped defected ground structure for coplanar waveguide," *IEEE Microwave and Wireless Components Letters*, vol. 12, no. 9, pp. 330-332, 2002.
- [74] S. Gao, L. W. Li, M. S. Leong, and T. S. Yeo, "A broad-band dual-polarized microstrip patch antenna with aperture coupling," *IEEE Transactions on Antennas and Propagation*, vol. 51, no. 4, pp. 898-900, 2003.
- [75] M. W. Young, S. Yong, and J. T. Bernhard, "A Miniaturized Frequency Reconfigurable Antenna With Single Bias, Dual Varactor Tuning," *IEEE Transactions on Antennas and Propagation*, vol. 63, no. 3, pp. 946-951, 2015.
- [76] M. A. S. Alkanhal, and A. F. Sheta, "A novel dual-band reconfigurable square-ring microstrip antenna," *Progress In Electromagnetics Research C*, vol. 70, pp. 337-49, 2007.
- [77] J. A. Zammit and A. Muscat, "A small tunable antenna using multiple shorting posts and varactor diodes," in *2008 3rd International Symposium on Communications, Control and Signal Processing*, pp. 83-86, 2008.

List of Publications

M. Al Ahmad, S. Kabeer and L. J. A. Olule, "Wireless Multiplexing Agile Antenna-Based Control System," *IEEE Access*, vol. 9, pp. 9664-9669, 2021

M. Al Ahmad, S. Kabeer, A. A. Sanad, and L. J. A. Olule, "Compact single-varactor diode frequency-reconfigurable microstrip patch antenna". *IET Microwaves Antennas and Propagation*, vol. 15, no. 9, pp. 1100-1107, 2021